

Dear Marcel van der Meer,
thank you very much for your constructive comments encouraging revision and restructuring of our manuscript. We considered all your comments carefully and we believe that our revised manuscript now clearly addresses all your requests. Please find below our responses (regular fonts) to your comments (bold fonts).

First of all I would like to thank both reviewers for reviewing this manuscript and you for your reply. I think the reviewers made some good suggestions concerning your manuscript and I think you should definitely address these.

- We addressed all questions and comments raised by both reviewers (see response letters and modified manuscripts uploaded to the discussion forum in February and May 2019, respectively) and are confident that our revisions satisfy their requests. While revising our manuscript again to address the editor's most recent recommendations, previous modifications suggested by the reviewers are still valid.

There are two main issues I think you really need to address. The first issue deals with the analytical details. In response to my earlier comments you have already addressed some. I assume that when silylating sterols you added both BSTFA and pyridine, for instance?

- We note that the addition of pyridine for sterol silylation is not part of our (and e.g. Simon Belt's) analytical protocol. We revised the methods section (section 3.2) and added references for our laboratory analyses. We note that our sterol treatment and analysis follow the procedure outlined in Belt et al. (2013) and Stein et al. (2012) to ensure comparability of the results obtained within different laboratories.

Another question I have related to analytical details is if you could give a more thorough description on how you calibrated the HBI response on the MS in order to be able to compare them with other compounds?

- We revised this in section 3.2 and added information on the determination of instrumental response factors by means of a standard sediment with known (GC-FID determined) HBI concentrations. We now also include details on the HBI identification and quantification in the supplementary material.

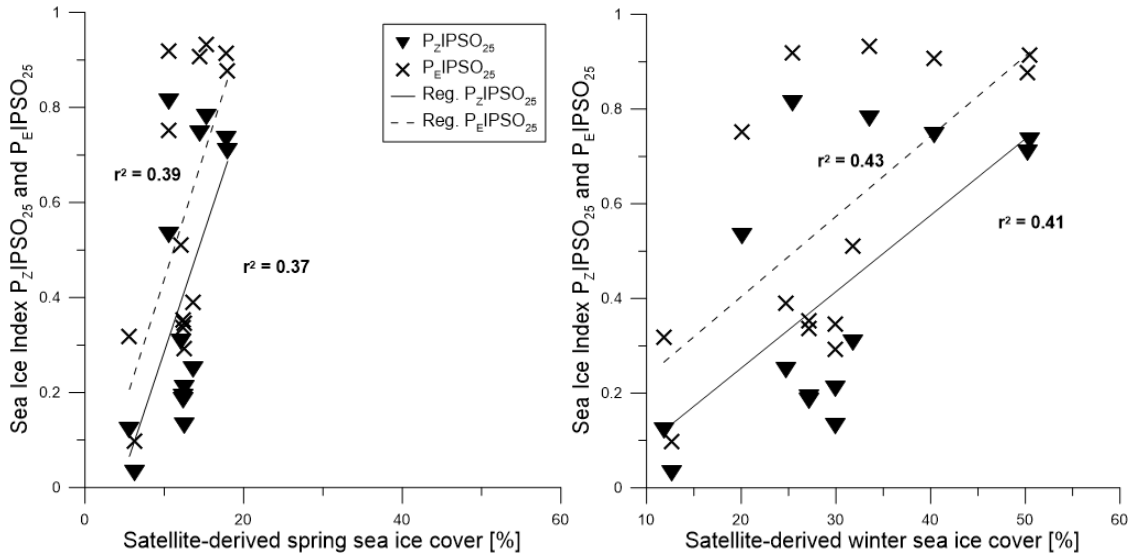
How does this affect the use of the c-factor, sometimes you use it, sometimes you do.

- Previously, the so-called c-factor has been introduced to account for the normally much higher concentrations of phytosterols compared to HBI concentrations. Considering this factor for the calculation of sterol-based PIP25/PIPSO25 indices clearly facilitates their comparison with HBI-triene-based PIP25/PIPSO25 indices (using a c-factor of 1; Smik et al., 2016). Sterol-based PIP25/PIPSO25 values determined without a c-factor would be orders of magnitude lower. We rephrased the sections commenting on the application of the c-factor within the methods section (3.2) and now provide references on (ongoing) discussions on the application of the c-factor (e.g., Smik et al. (2016), Müller et al. (2011) and Belt and Müller (2013)).

There is a relatively large number of “zero” points, how does this affect your correlations?

- Most of these “zero points” relate to sampling stations in the Drake Passage, where the absence of IPSO25 (and PIPSO25 values of zero) are in accordance with the absence of sea ice. We comment on the absence of IPSO25 at two core sites off the continental slope which (according to satellite data) experience sea ice cover in section 4.2. We relate the absence of IPSO25 at these sites to e.g. the environmental preferences of its

source diatom *Berkeleya adeliensis* (restricted to landfast/platelet ice). Accordingly, also PIPSO25 values are zero at these sites (suggesting ice-free conditions). For the correlation of biomarker data (+ PIPSO25 values) with satellite data, we follow earlier studies (Müller et al., 2011; Navarro-Rodriguez et al., 2012; Smik et al., 2016; Xiao et al., 2015) and argue that “zero points” referring to the absence of sea ice should not be excluded (in our study, omitting these “zero points” would lead to weaker correlations; see PIPSO25 correlations with spring and winter sea ice below).



How do you deal with the large variability or standard deviation in your sea ice concentration?

- We now comment on the high standard deviation in the satellite-derived sea ice concentrations in the method section 3.4 and consider that the use of mean averages facilitates the comparison with sedimentary data (integrating and reflecting a significantly longer time interval of variable sea ice conditions).

My second issue has to do with the set-up of the manuscript. You now discuss the data in light of your new sea ice proxy PIPSO25, the alternative would be to discuss your data in light of all the environmental parameters including sea ice and end with by suggesting a potential new sea ice proxy for the Antarctic region, PIPSO25. Basically reorganizing the discussion to a more general discussion rather than the focus on the proxy. The data you have generated is clearly interesting, the issues are with the PIPSO proxy, by shifting the focus you would generate a more acceptable manuscript. It might be that the oceanographic setting around Antarctica is so complex that a sea ice proxy similar to the Arctic is just not feasible, for instance. When discussing your data in light of the oceanography, sea ice extend and other environmental parameters this outcome would be fine. In the current manuscript with the focus on the PIPSO25 proxy, the proxy has to work, any other conclusion cannot not be accepted. I think this is why the manuscript as is feels a bit forced, PIPSO25 has to work and this is not necessary.

- We agree with the editor and restructured the results/discussion chapters as recommended. First, we now present and discuss the distribution of biomarkers in the light of sea surface conditions (i.e. oceanographic features; primary productivity; (potential) source organisms for the individual lipids). These sections are now followed by a comparison of the biomarker distribution patterns with satellite sea ice

data and diatom-based sea ice estimates. In the final results/discussion chapter (4.4) we now present and discuss the adaptation of the Arctic Ocean PIP25-approach using IPSO25 for calculating the PIPSO25 index. We now also comment on the role that platelet ice formation plays for the distribution of IPSO25 and the potential application of PIPSO25. Clearly, the sea ice environment in the Southern Ocean differs from the Arctic Ocean and these limitations have to be considered for an attempt to adopt the semi-quantitative PIP25 approach. We now emphasize these limitations in the manuscript.

Please also check if you site all relevant literature, also the more recent publications and in the right place.

- We revised and updated the literature data base and now also include most recently published papers.

Again, with a slightly different focus I think you have a great dataset and a very interesting manuscript. I am looking forward to your rebuttal and revised manuscript.

- We are very glad that you appreciate our work and hope that our recent revisions fulfill your expectations.

References

- Belt, S. T., Brown, T. A., Ringrose, A. E., Cabedo-Sanz, P., Mundy, C. J., Gosselin, M., and Poulin, M., 2013, Quantitative measurement of the sea ice diatom biomarker IP25 and sterols in Arctic sea ice and underlying sediments: Further considerations for palaeo sea ice reconstruction: *Organic Geochemistry*, v. 62, p. 33-45.
- Belt, S. T., and Müller, J., 2013, The Arctic sea ice biomarker IP₂₅: a review of current understanding, recommendations for future research and applications in palaeo sea ice reconstructions: *Quaternary Science Reviews*, v. 79, no. 1, p. 9-25.
- Müller, J., Wagner, A., Fahl, K., Stein, R., Prange, M., and Lohmann, G., 2011, Towards quantitative sea ice reconstructions in the northern North Atlantic: A combined biomarker and numerical modelling approach: *Earth and Planetary Science Letters*, v. 306, no. 3-4, p. 137-148.
- Navarro-Rodriguez, A., Belt, S. T., Knies, J., and Brown, T. A., 2012, Mapping recent sea ice conditions in the Barents Sea using the proxy biomarker IP25: implications for palaeo sea ice reconstructions: *Quaternary Science Reviews*, v. 79, no. 1, p. 26-39.
- Smik, L., Cabedo-Sanz, P., and Belt, S. T., 2016, Semi-quantitative estimates of paleo Arctic sea ice concentration based on source-specific highly branched isoprenoid alkenes: A further development of the PIP25 index: *Organic Geochemistry*, v. 92, p. 63-69.
- Stein, R., Fahl, K., and Müller, J., 2012, Proxy reconstruction of Cenozoic Arctic Ocean sea-ice history: From IRD to IP25: *Polarforschung*, v. 82, no. 1, p. 37-71.
- Xiao, X., Fahl, K., Müller, J., and Stein, R., 2015, Sea-ice distribution in the modern Arctic Ocean: Biomarker records from trans-Arctic Ocean surface sediments: *Geochimica et Cosmochimica Acta*, v. 155, p. 16-29.

Formatiert: Kopfzeile

Formatvorlagendefinition: Standard: Zeilenabstand: Doppelt

Formatvorlagendefinition: Überschrift 3: Schriftart: Times New Roman, 10 Pt., Fett, Schriftfarbe: Text 1, Zeilenabstand: Doppelt

Formatiert: Zeilenabstand: einfach

Gelöscht: semi-quantitative

Gelöscht: The

Gelöscht: diatoms seem

Gelöscht: . We here propose and evaluate the combination of IPSO₂₅ with a more unsaturated highly branched isoprenoid alkene and phytosterols and introduce the PIPSO₂₅ index as a potentially semi-quantitative sea ice proxy. This organic geochemical approach

Gelöscht: complemented with diatom data. PIPSO₂₅ sea ice estimates are used to discriminate between areas characterized by permanently ice-free conditions, seasonal sea ice cover and extended sea ice cover. These trends are consistent with satellite sea ice data and winter sea ice concentrations estimated by diatom transfer functions. Minor offsets between proxy-based

Formatiert: Nicht Hervorheben

Highly branched isoprenoids for Southern Ocean sea ice reconstructions: a pilot study from the Western Antarctic Peninsula

Maria-Elena Vorrath¹, Juliane Müller^{1,2,3}, Oliver Esper¹, Gesine Mollenhauer^{1,2}, Christian Haas¹, Enno Schefuß², Kirsten Fahl¹

¹Alfred Wegener Institute, Helmholtz Centre for Polar and Marine Research, Bremerhaven, Germany

²MARUM – Center for Marine Environmental Sciences, University of Bremen, Germany

³Department of Geosciences, University of Bremen, Germany

Correspondence to: Maria-Elena Vorrath, maria-elena.vorrath@awi.de

Abstract. Organic geochemical and micropaleontological analyses of surface sediments collected in the southern Drake Passage and the Bransfield Strait, Antarctic Peninsula, enable a proxy-based reconstruction of recent sea ice conditions in this climate sensitive area. We study the distribution of the sea ice biomarker IPSO₂₅, and biomarkers of open marine environments such as more unsaturated highly branched isoprenoid alkenes and phytosterols. Comparison of the sedimentary distribution of these biomarker lipids with sea ice data obtained from satellite observations and diatom-based sea ice estimates provide for an evaluation of the suitability of these biomarkers to reflect recent sea surface conditions. The distribution of IPSO₂₅ supports earlier suggestions that the source diatom seems to be common in near-coastal environments characterized by an annually recurring sea ice cover, while the distribution of the other biomarkers is highly variable. Offsets between sea ice estimates deduced from the abundance of biomarkers and satellite-based sea ice data are attributed to the different time intervals recorded within the sediments and the instrumental records from the study area, which experienced rapid environmental changes during the past 100 years. To distinguish areas characterized by permanently ice-free conditions, seasonal sea ice cover and extended sea ice cover, we apply the concept of the PIP₂₅ index from the Arctic Ocean on our data and introduce the term PIPSO₂₅ as a potential sea ice proxy. While the trends in PIPSO₂₅ are generally consistent with satellite sea ice data and winter sea ice concentrations estimated by diatom transfer functions, more studies on the environmental significance of IPSO₂₅ as a Southern Ocean sea ice proxy are needed before this biomarker can be applied for semi-quantitative sea ice reconstructions.

Formatiert: Kopfzeile

1

2 Key Words: biomarker, IPSO₂₅, sea ice, Bransfield Strait, satellite observation

3 1 Introduction

4 In the last century, the Western Antarctic Peninsula (WAP) has undergone a rapid warming of the atmosphere of

Formatiert: Zeilenabstand: einfach

5 $3.7 \pm 1^\circ \text{C}$, which exceeds several times the average global warming (Pachauri et al., 2014; Vaughan et al., 2003).

Gelöscht: (Vaughan et al., 2003)

6 Simultaneously, a reduction in sea ice coverage (Parkinson and Cavalieri, 2012), a shortening of the sea ice season
7 (Parkinson, 2002) and a decreasing sea ice extent of ~4-10 % per decade (Liu et al., 2004) are recorded in the
8 adjacent Bellingshausen Sea. The loss of seasonal sea ice and increased melt water fluxes impact the formation of
9 deep and intermediate waters, the ocean-atmosphere-exchange of gases and heat, the primary production and

10 higher trophic levels (Arrigo et al., 1997; Mendes et al., 2013; Morrison et al., 2015; Orsi et al., 2002; Rintoul,
11 2007). Since the start of satellite-based sea ice observations, however, a slight increase in total Antarctic sea ice
12 extent has been documented, which contrasts the significant decrease of sea ice in Western Antarctica, especially
13 around the WAP (Hobbs et al., 2016).

Gelöscht: (Arrigo et al., 1997; Morrison et al., 2015; Orsi et al., 2002; Rintoul, 2007)

14 For an improved understanding of the oceanic and atmospheric feedback mechanisms associated with the observed
15 changes in sea ice coverage, reconstructions of past sea ice conditions in climate sensitive areas such as the WAP
16 are of increasing importance. A common approach for sea ice reconstructions in the Southern Ocean is based on
17 the investigation of sea ice associated diatom assemblages preserved in marine sediments (Bárcena et al., 1998;
18 Gersonde and Zielinski, 2000; Heroy et al., 2008; Leventer, 1998; Minzoni et al., 2015). By means of transfer
19 functions, this approach can provide quantitative estimates of a paleo sea ice coverage (Crosta et al., 1998; Esper
20 and Gersonde, 2014a). The application of diatoms for paleoenvironmental studies, however, can be limited by the
21 selective dissolution of biogenic opal frustules (Burckle and Cooke, 1983; Esper and Gersonde, 2014b) in the
22 photic zone (Ragueneau et al., 2000) and in surface sediments (Leventer, 1998). As an alternative or additional
23 approach to diatom studies, Massé et al. (2011) proposed the use of a specific biomarker lipid – a diunsaturated
24 highly branched isoprenoid alkene (HBI C_{25:2}, Fig. 1) – for Southern Ocean sea ice reconstructions. The HBI diene
25 was first described by Nichols et al. (1988) from sea ice diatoms. ¹³C isotopic analyses of the HBI diene suggest a
26 sea ice origin for this molecule (Sinninghe Damsté et al., 2007; Massé et al., 2011) and this is further corroborated
27 by the identification of the sea ice diatom *Berkeleya adeliensis* as a producer of this HBI diene (Belt et al., 2016).

28 *Berkeleya adeliensis* is associated with Antarctic landfast ice and the underlying so-called platelet ice (Riaux-
29 Gobin and Poulin, 2004). In a survey of surface sediments collected from proximal sites around Antarctica, Belt
30 et al. (2016) note a widespread sedimentary occurrence of the HBI diene and – by analogy with the Arctic HBI

Formatiert: Kopfzeile

1 monoene termed IP₂₅ (Belt et al., 2007) – proposed the term IPSO₂₅ (Ice Proxy for the Southern Ocean with 25
2 carbon atoms) as a new name for this biomarker.

3 In previous studies, an HBI triene (HBI C_{25:3}; Fig. 1) found in polar and sub-polar phytoplankton samples (Massé
4 et al., 2011) has been considered alongside IPSO₂₅ and the ratio of IPSO₂₅ to this HBI triene hence has been
5 interpreted as a measure for the relative contribution of organic matter derived from sea ice algae versus open
6 water phytoplankton (Massé et al., 2011; Collins et al., 2013; Etourneau et al., 2013; Barbara et al., 2013, 2016).

7 Collins et al. (2013) further suggested that the HBI triene might reflect phytoplankton productivity in marginal ice
8 zones (MIZ) and, based on the observation of elevated HBI triene concentrations in East Antarctic MIZ surface
9 waters, this has been strengthened by Smik et al. (2016a). Known source organisms of HBI trienes (Fig. 1 shows

Gelöscht: C_{25:3}

10 molecular structures of both the E- and Z-isomer) are, for example, *Rhizosolenia* and *Pleurosigma* diatom species
11 (Belt et al., 2000, 2017). In the subpolar North Atlantic, the HBI Z-triene has been used to further modify the so-
12 called PIP₂₅ index (Smik et al., 2016b) - an approach for semi-quantitative sea ice estimates. Initially, PIP₂₅ was

13 based on the employment of phytoplankton-derived sterols, such as brassicasterol (24-methylcholesta-5,22E-dien-
14 3β-ol) and dinosterol (4α,23,24-trimethyl-5α-cholest-22E-en-3β-ol) (Kanazawa et al., 1971; Volkman, 2003), to
15 serve as open-water counterparts, while IP₂₅ reflects the occurrence of a former sea ice cover (Belt et al., 2007;
16 Müller et al., 2009, 2011). Consideration of these different types of biomarkers helps to discriminate between ice-

Gelöscht: (for further details see Belt, 2018; Belt and Müller, 2013a).

17 free and permanently ice-covered ocean conditions, both resulting in a lack of IP₂₅ and IPSO₂₅, respectively (for
18 further details see Belt, 2018; Belt and Müller, 2013). Uncertainties in the source-specificity of brassicasterol
19 (Volkman, 1986) and its identification in Arctic sea ice samples, however, require caution when pairing this sterol

Gelöscht: (Belt et al., 2013),

20 with a sea ice biomarker lipid for Arctic sea ice reconstructions, (Belt et al., 2013). In this context, we note that
21 Belt et al. (2018) reported that brassicasterol is not evident in the IPSO₂₅ producing sea ice diatom *Berkeleya*
22 *adeliensis*. While the applicability of HBIs (and sterols) to reconstruct past sea ice conditions has been thoroughly
23 investigated in the Arctic Ocean (Belt, 2018; Stein et al., 2012; Xiao et al., 2015), only two studies document the
24 distribution of HBIs in Southern Ocean surface sediments (Belt et al., 2016; Massé et al., 2011). The circum-
25 Antarctic data set published by Belt et al. (2016), however, does neither report HBI triene nor sterol abundances.

Gelöscht: not

26 Significantly more studies so far focused on the use of IPSO₂₅ and the HBI Z-triene for paleo sea ice
27 reconstructions and these records are commonly compared to micropaleontological diatom analyses (e.g., Barbara
28 et al., 2013; Collins et al., 2013; Denis et al., 2010).

29 Here, we provide a first overview of the distribution of IPSO₂₅, HBI trienes, brassicasterol and dinosterol in surface
30 sediments from the permanently ice-free ocean in the Drake Passage towards the seasonal sea ice inhabited area
31 of the Bransfield Strait at the northern WAP. Sea ice estimates based on biomarkers are compared to sea ice

Gelöscht: northern part of the WAP (southern Drake Passage and Bransfield Strait). These biomarker data are completed by diatom analyses and remote sensing sea ice data.

Formatiert: Kopfzeile

1 [concentrations derived from diatom transfer functions and satellite-derived data on the recent sea ice conditions in](#)
2 [the study area](#). We further introduce and discuss the so-called PIPSO₂₅ index (phytoplankton-IPSO₂₅ index),
3 which, following the PIP₂₅ approach in the Arctic Ocean (Müller et al., 2011), may serve as a [further](#) indicator of
4 past Southern Ocean sea ice cover.

Gelöscht: semi-quantitative

Gelöscht: These biomarker-based sea ice estimates are compared to sea ice concentrations derived from diatom transfer functions and satellite-derived data on the recent sea ice conditions in the study area.

Formatiert: Schriftart: Times New Roman, Nicht Fett, Schriftfarbe: Automatisch

Formatiert: Kopfzeile

Formatiert: Zeilenabstand: einfach

Gelöscht: While the

Gelöscht:), a complex current system prevails in the Bransfield Strait. According to Sangrà et al. (2011) a branch of the ACC enters the Bransfield Strait in the west as the Bransfield Current, carrying transitional waters under the influence of the Bellingshausen Sea (Transitional Bellingshausen Sea Water, TBW).

Formatiert: Englisch (Vereinigtes Königreich)

2 Oceanographic setting

The study area includes the southern Drake Passage and the Bransfield Strait located between the South Shetland Islands and the northern tip of the WAP (Fig. 2a and b). The oceanographic setting in the Drake Passage is dominated by the Antarctic Circumpolar Current (ACC) and several oceanic fronts showing large geostrophic water mass flows and subduction and upwelling of water masses (Orsi et al., 1995). The Antarctic Polar Front (APF) divides relatively warm subantarctic waters from the cold and salty Antarctic waters, while the southern Antarctic Circumpolar Current Front (SACCF) often associates with the maximum sea ice extent (Kim and Orsi, 2014). The current system in the Bransfield Strait is relatively complex and the mixture of water masses is not yet well understood (Moffat and Meredith, 2018; Sangrà et al., 2011). A branch of the ACC enters the Bransfield Strait in the west as the Bransfield Current, carrying transitional waters under the influence of the Bellingshausen Sea (Transitional Bellingshausen Sea Water, TBW). The TBW is characterized by a well-stratified, fresh and warm water mass with summer sea surface temperatures (SST) above 0° C. Below the shallow TBW, a narrow tongue of circumpolar deep water (CDW) flows along the slope of the South Shetland Islands (Sangrà et al., 2011). In the eastern part, transitional water from the Weddell Sea (Transitional Weddell Sea Water, TWW) enters the Bransfield Strait through the Antarctic Sound and from the Antarctic Peninsula (AP). This water mass corresponds to the Antarctic Coastal Current (Collares et al., 2018; Thompson et al., 2009). The TWW is significantly colder (summer SST < 0° C) and saltier due to extended sea ice formation in the Weddell Sea Gyre. The two water masses are separated at the sea surface by the Peninsula Front characterized by a TBW anticyclonic eddy system (Sangrà et al., 2011). While the TWW occupies the deep water column of the Bransfield Strait (Sangrà et al., 2011), it joins the surface TBW in the southwestern Bransfield Strait (Collares et al., 2018).

Due to high concentrations of dissolved iron on the shelf (Klunder et al., 2014), the area around the WAP is characterized by a high primary production with high vertical export fluxes during early summer associated with the formation of fast sinking mineral aggregates and fecal pellets (Kim et al., 2004; Wefer et al., 1988). The Peninsula Front divides the Bransfield Strait into two biogeographic regimes of high chlorophyll and diatom abundance in the TBW and low chlorophyll values and a pre-dominance of nanoplankton in the TWW (Gonçalves-Araujo et al., 2015), which is also reflected in the geochemistry of surface sediments (Cárdenas et al., 2018).

Formatiert: Kopfzeile

3 Materials and Methods

3.1 Sediment Samples and radiocarbon dating

In total, 26 surface sediment samples obtained by multicorers and box corers during the RV *Polarstern* cruise PS97 (Lamy, 2016) were analyzed (Fig. 2, Table 1). All samples were stored frozen and in glass vials. The composition of the sediments ranges from foraminiferal mud in the Drake Passage to diatomaceous mud with varying amounts of ice rafted debris in the Bransfield Strait (Lamy, 2016). ¹⁴C radiocarbon dating of two samples from the PS97 cruise and one from the *Polarstern* cruise ANT-VI/2 (Fütterer, 1988) was conducted using the mini carbon dating system (MICADAS) at the Alfred Wegener Institute (AWI) in Bremerhaven, Germany, following the method of Wacker et al. (2010). The ¹⁴C ages were calibrated to calendar years before present (cal BP) using the Calib 7.1 software (Stuiver et al., 2019) with an estimated reservoir age of 1178 years, derived from the six closest reference points listed in the Marine Reservoir Correction Database (www.calib.org).

Formatiert: Zeilenabstand: einfach

3.2 Organic geochemical analyses

For biomarker analyses, sediments were freeze-dried and homogenized using an agate mortar. After freeze-drying, samples were stored frozen to avoid degradation. The extraction, purification and quantification of HBIs and sterols follow the analytical protocol applied by the international community of researchers performing HBI and sterol-based sea ice reconstructions (Belt et al., 2013, 2014; Stein et al., 2012). Prior to extraction, internal standards 7-hexylnonadecane (7-HND) and 5 α -androstan-3 β -ol were added to the sediments. For the ultrasonic extraction (15 min), a mixture of CH₂Cl₂:MeOH (v/v 2:1; 6 ml) was added to the sediment. After centrifugation (2500 rpm for 1 min), the organic solvent layer was decanted. The ultrasonic extraction step was repeated twice. From the combined total organic extract, apolar hydrocarbons were separated via open column chromatography (SiO₂) using hexane (5 ml). Sterols were eluted with ethylacetate:hexane (v/v 20:80; 8 ml). HBIs were analyzed using an Agilent 7890B gas chromatography (30 m DB 1MS column, 0.25 mm diameter, 0.250 μ m film thickness, oven temperature 60° C for 3 min, rise to 325° C within 23 min, holding 325° C for 16 min) coupled to an Agilent 5977B mass spectrometer (MSD, 70 eV constant ionization potential, ion source temperature 230° C). Sterols were first silylated (200 μ l BSTFA; 60° C; 2 hours; Belt et al., 2013; Brault and Simoneit, 1988; Fahl and Stein, 2012) and then analyzed on the same instrument using a different oven temperature program (60° C for 2 min, rise to 150° C within 6 min, rise to 325° C within 56 min 40 sec). As recommended by Belt (2018), the identification of IPSO₂₅ and HBI trienes is based on comparison of their mass spectra with published mass spectra (Belt, 2018; Belt et al., 2000; see supplementary material S1). Regarding the potential sulfurization of IPSO₂₅, we examined

Gelöscht: Also after

Formatiert: Zeilenabstand: einfach

Gelöscht: (Belt et al., 2014; Stein et al., 2012)

Gelöscht: 6ml

Gelöscht: Sterols were first silylated (200 μ l BSTFA; 60° C; 2hours) and then analyzed on the same instrument using a different oven temperature program (60° C for 2 min, rise to 150° C within 6 min, rise to 325° C within 56 min 40 sec).

Gelöscht: (Belt et al., 2000).

1 the GC-MS chromatogram and mass spectra of each sample for the occurrence of the HBI C₂₅ sulfide (Sinninghe
2 Damsté et al., 2007). The C₂₅ HBI thiane was absent in all samples. For the quantification, manually integrated
3 peak areas of the molecular ions of the HBIs in relation to the fragment ion m/z 266 of 7-HND were used.
4 Instrumental response factors are determined by means of an external standard sediment from the Lancaster Sound,
5 Canada. The HBI concentrations in this sediment are known and a set of calibration series was applied to determine
6 the different response factors of the HBI molecular ions (m/z 346; m/z 348) and the fragment ion of 7-HND (m/z
7 266) (supplement S2; Belt, 2018; Fahl and Stein, 2012). The identification of sterols was based on comparison of
8 their retention times and mass spectra with those of reference compounds run on the same instrument. Comparison
9 of peak areas of individual analytes and the internal standard was used for sterol quantification. The error
10 determined by duplicate GC-MS measurements was below 0.7%. The detection limit for HBIs and sterols was
11 0.5 ng/g sediment. Absolute concentrations of HBIs and sterols were normalized to total organic carbon contents
12 (for TOC data see Cárdenas et al., 2018).

13 The herein presented phytoplankton-IPSO₂₅ index (PIPSO₂₅) is calculated using the same formula as for the PIP₂₅
14 index following Müller et al. (2011):

$$15 \text{PIPSO}_{25} = \frac{\text{IPSO}_{25}}{\text{IPSO}_{25} + (c \times \text{phytoplankton marker})} \quad (1)$$

16 The balance factor c (c = mean IPSO₂₅ / mean phytoplankton biomarker) is applied to account for the high offsets
17 in the magnitude of IPSO₂₅ and sterol concentrations (see Belt and Müller, 2013; Müller et al., 2011; Smik et al.,
18 2016b for details and a discussion of the c-factor). Since the concentrations of IPSO₂₅ and both HBI trienes are in
19 the same range, the c-factor has been set to 1 (following Smik et al., 2016b). For the calculation of the sterol-based
20 PIPSO₂₅ index using brassicasterol and dinosterol the applied c-factor is 0.0048 and 0.0137, respectively.

21 Stable carbon isotope composition of IPSO₂₅, requiring a minimum of 50 ng carbon, was successfully determined
22 on five samples using GC-irm-MS. The ThermoFisher Scientific Trace GC was equipped with a 30 m Restek Rxi-
23 5 ms column (0.25 mm diameter, 0.25 µm film thickness) and coupled to a Finnigan MAT 252 isotope ratio mass
24 spectrometer via a modified GC/C interface. Combustion of compounds was done under continuous flow in
25 ceramic tubes filled with Ni wires at 1000° C under an oxygen trickle flow. The same GC program as for the HBI
26 identification was used. The calibration was done by comparison to a CO₂ reference gas. The values of δ¹³C are
27 expressed in per mill (‰) against Vienna PeeDee Belemnite (VPDB) and the mean standard deviation was <0.9
28 ‰. An external standard mixture was measured every six runs, achieving a long-term mean standard deviation of
29 0.2‰ and an average accuracy of <0.1 ‰. Stable isotopic composition of neither HBI trienes nor sterols could be
30 determined due to coeluting compounds.

Formatiert: Kopfzeile

Gelöscht: those

Gelöscht: An

Gelöscht: calibration for HBI diene and trienes was applied using a sample with known HBI concentrations

Gelöscht: ,

Gelöscht: account for

Gelöscht:).

Gelöscht: The balance factor c (c = mean IPSO₂₅ / mean phytoplankton biomarker) is applied to account for the high offsets in the magnitude of IPSO₂₅ and sterol concentrations.

Formatiert: Zeilenabstand: einfach

Gelöscht: 30m

Formatiert: Kopfzeile

Formatiert: Zeilenabstand: einfach

1

2 3.3 Diatoms

3 Details of the standard technique of diatom sample preparation were developed in the micropaleontological
4 laboratory at the Alfred Wegener Institute (AWI) in Bremerhaven, Germany. The preparation included a treatment
5 of the sediment samples with hydrogen peroxide and concentrated hydrochloric acid to remove organic and
6 calcareous remains. After washing the samples several times with purified water, the water was removed and the
7 diatoms were embedded on permanent mounts for counting (see detailed description by Gersonde and Zielinski,
8 2000). The respective diatom counting was carried out according to Schrader and Gersonde (1978). On average,
9 400 to 600 diatom valves were counted in each slide using a Zeiss Axioplan 2 at x1000 magnification. In general
10 preservation state of the diatom assemblages was moderate to good in the Bransfield Strait and decreased towards
11 the Drake Passage where it is moderate to poor.

12 Diatoms were identified to species or species group level and if possible to forma or variety level. The taxonomy
13 follows primarily Hasle and Syvertsen (1996), Zielinski and Gersonde (1997), and Armand and Zielinski (2001).
14 Following Zielinski and Gersonde (1997) and Zielinski et al. (1998) we combined some taxa to groups:

15 The *Thalassionema nitzschioides* group combines *T. nitzschioides* var. *lanceolata* and *T. nitzschioides* var.
16 *capitulata*, two varieties with gradual transition of features between them and no significantly different ecological
17 response. The species *Fragilariopsis curta* and *Fragilariopsis cylindrus* were combined as *F. curta* group taking
18 into account their similar relationship to sea ice and temperature (Armand et al., 2005; Zielinski and Gersonde,
19 1997). Furthermore, the *Thalassiosira gracilis* group comprises *T. gracilis* var. *gracilis* and *T. gracilis* var. *expecta*
20 because the characteristic patterns in these varieties are often transitional, which hampers distinct identification.

21 Although the two varieties *Eucampia antarctica* var. *recta* and *E. antarctica* var. *antarctica* display different
22 biogeographical distribution (Fryxell and Prasad, 1990), they were combined to the *E. antarctica* group. This
23 group was not included in the transfer function (TF) as it shows no relationship to either sea ice or temperature
24 variation (Esper and Gersonde, 2014a, b). Besides the *E. antarctica* group, we also discarded diatoms assembled
25 as *Chaetoceros* spp. group from the TF-based re-constructions, following Zielinski et al. (1998) and Esper and
26 Gersonde (2014a). This group combines mainly resting spores of a diatom genus with a ubiquitous distribution
27 pattern that cannot be identified to species level due to the lack of morphological features during light microscopic
28 inspection. Therefore, different ecological demands of individual taxa cannot be distinguished.

29 For estimating winter sea ice (WSI) concentrations we applied the marine diatom TF MAT-D274/28/4an,
30 comprising 274 reference samples from surface sediments in the western Indian, the Atlantic and the Pacific
31 sectors of the Southern Ocean, with 28 diatom taxa and taxa groups, and an average of 4 analogs (Esper and

Formatiert: Kopfzeile

1 Gersonde, 2014a). The WSI estimates refer to September sea-ice concentrations averaged over a time period from
2 1981 to 2010 at each surface sediment site (National Oceanic and Atmospheric Administration, NOAA; Reynolds
3 et al., 2002, 2007). The reference data set is suitable for our approach as it uses a 1° by 1° grid, representing a
4 higher resolution than previously used and results in a root mean squared error of prediction (RMSEP) of 5.52%
5 (Esper and Gersonde, 2014a). We defined 15% concentration as threshold for maximum sea-ice expansion
6 following the approach of Zwally et al. (2002) for the presence or absence of sea ice, and 40% concentration
7 representing the average sea-ice edge (Gersonde et al., 2005; Gloersen et al., 1993). MAT calculations were carried
8 out with the statistical computing software R (R Core Team, 2012) using the additional packages Vegan (Oksanen
9 et al., 2012) and Analogue (Simpson and Oksanen, 2012). Further enhancement of the sea-ice reconstruction was
10 obtained by consideration of the abundance pattern of the diatom sea-ice indicators allowing for qualitative
11 estimate of sea-ice occurrence, as proposed by Gersonde and Zielinski (Gersonde and Zielinski, 2000).

13 3.4 Sea ice data

14 The mean monthly satellite sea ice concentration was derived from Nimbus-7 SMMR and DMSP SSM/I-SSMIS
15 passive microwave data and downloaded from the National Snow and Ice Data Center (NSIDC; Cavalieri et al.,
16 1996). The sea ice concentration is expressed to range from 0 to 100 %, with concentrations below 15 %
17 suggesting the minor occurrence of sea ice. Accordingly, the sea ice extent is defined as the ocean area with a sea
18 ice cover of at least 15 %.
19 An interval from 1980 to 2015 was used to generate an average sea ice distribution for each season: spring (SON),
20 summer (DJF), autumn (MAM) and winter (JJA) (Table 2) and the data is considered to reflect the modern mean
21 state of sea ice coverage around the WAP. The high standard deviation in the seasonal sea ice concentrations (up
22 to 26 % in winter; Table 2) in the vicinity of the WAP is attributed to the distinct intra- and interannual variability
23 in sea ice coverage. In this regard, Kim et al. (2005) already related interannual changes in particle flux to annual
24 changes in sea ice cover in the Bransfield Strait. We here suggest that by considering mean sea ice concentrations
25 determined for an observational period of 35 years, reflects a good estimate of average sea ice conditions and
26 facilitates the comparison with sedimentary archives.

Formatiert: Zeilenabstand: einfach

Gelöscht: An interval from 1980 to 2015 was used to generate an average sea ice distribution for each season, spring (SON), summer (DJF), autumn (MAM) and winter (JJA).

Formatiert: Kopfzeile

4 Results and Discussion

In the following we present and discuss the sedimentary concentrations of IPSO₂₅, HBI trienes and phytosterols regarding their spatial distribution patterns in relation to the environmental conditions and oceanographic features in the study area. We especially focus on the applicability of these biomarkers for reconstructing sea ice conditions and integrate information derived from satellite observations and diatom-based sea ice estimations. We further discuss the possible approach of a sea ice index PIPSO₂₅ by analogy with the Arctic sea ice index PIP₂₅ (Müller et al., 2011).

4.1 Biomarker distributions in surface sediments

Distribution of IPSO₂₅

The sea ice biomarker IPSO₂₅ was detected in 14 samples, with concentrations ranging between 0.37 and 17.81 µg g⁻¹ TOC (Table 1). The distribution of IPSO₂₅ in the study area shows a clear northwest-southeast gradient (Fig. 3a) with concentrations increasing from the continental slope and around the South Shetland Islands towards the continental shelf. Maximum IPSO₂₅ concentrations are observed at stations under TWW influence with distinctly cold summer SSTs in the Bransfield Strait. According to Belt et al. (2016), deposition of IPSO₂₅ is highest in areas covered by landfast sea ice and platelet ice during early spring and summer. Platelet ice is formed under supercooling ocean conditions in the vicinity of ice-shelves and subsequently may be incorporated into drifting sea ice (Gough et al., 2012; Hoppmann et al., 2015). We note that, for example, core sites PS97/068, PS97/069, PS97/072, and PS97/073 in the central and eastern Bransfield Strait are located too distal to be covered by fast ice and suggest that peak IPSO₂₅ concentrations at these sites may refer to the frequent drift and melt of sea ice exported from the Weddell Sea into the Bransfield Strait. The vertical export of biogenic material from sea ice towards the seafloor may be accelerated significantly by the formation of organic-mineral aggregates, fecal pellets or by (cryogenic) gypsum ballasting, which promotes a rapid burial and sedimentation of organic matter in polar settings (De La Rocha and Passow, 2007; Wefer et al., 1988; Wollenburg et al., 2018). A recent study from Schmidt et al. (2018) shows that the occurrence of IPSO₂₅ in suspended matter and pelagic grazers (krill) is closely linked to the position of the sea ice edge. Lateral subsurface advection of organic matter (including biomarkers) through the TWW, however, may also contribute to elevated IPSO₂₅ concentrations at these sites. IPSO₂₅ was not detected in sediments from the permanently ice-free areas in the Drake Passage. The δ¹³C values of IPSO₂₅ are between -10.3 ‰ and -14.7 ‰ which is the commonly observed range for IPSO₂₅ in surface sediments, sea ice derived organic matter, and in Antarctic krill stomachs (Belt et al., 2016; Massé et al., 2011; Schmidt et al., 2018). These values contrast the low δ¹³C values of marine phytoplankton lipids in

Formatiert: Schriftart: Kursiv

Gelöscht: , HBI trienes and sterols

Formatiert: Schriftart: Kursiv

Formatiert: Standard

Formatiert: Zeilenabstand: einfach

Gelöscht: The HBI Z-triene was present in all 26 samples (0.33-26.86 µg g⁻¹ TOC) and the HBI E-triene was found in 24 samples (0.15-13.87 µg g⁻¹ TOC). Brassicasterol was present in all measured samples with concentrations ranging from 3.39 to 5017.44 µg g⁻¹ TOC while dinosterol was detected in 22 samples (0.0002-1983.75 µg g⁻¹ TOC).

Gelöscht: area covered by landfast sea ice and platelet ice during early spring and summer. We suppose that core sites PS97/068 to

Gelöscht: Lateral subsurface advection of organic matter (incl. biomarkers) through the TWW, however, may also contribute to elevated IPSO₂₅ concentrations at these sites.

Formatiert: Schriftart: 12 Pt.

Gelöscht: IPSO₂₅ was not detected in sediments from the permanently ice-free areas in the Drake Passage.

Formatiert: Kopfzeile

Formatiert: Zeilenabstand: einfach

Gelöscht: rather

Gelöscht: (ocean temperature

Gelöscht: ¶

We observe higher concentrations of brassicasterol and dinosterol in the eastern part of the Drake Passage and, in contrast to the observation made for HBI trienes, also in the eastern and central Bransfield Strait (Fig. 3d and e). Dinosterol and, in particular, brassicasterol are known to have different source organisms including diatoms, dinoflagellates, prymnesiophycean algae and cyanobacteria (Volkman, 1986) and we assume that this diversity may account for the higher concentration of these lipids in Bransfield Strait sediments, while concentrations of HBI trienes, mainly derived from diatoms, are significantly lower. Sediments collected along the Hero Fracture Zone in the western Drake Passage (Fig. 2) contain only minor amounts of biomarkers except for elevated brassicasterol concentrations observed at stations PS97/048-1 and 049-2 (Fig. 3d). This part of the Drake Passage is mainly barren of fine-grained sediments and dominated by sands (Lamy, 2016), which may point to intensive winnowing by ocean currents impacting the deposition and burial of organic matter. We consider that also degradation of HBIs and sterols may affect their distribution within surface sediments. Rontani et al. (2014) report a higher sensitivity of tri-unsaturated HBIs to oxidation but also note that oxidation conditions in pelagic environments (i.e. their source organisms' habitat) are not as significant as those within sea ice. A more recent study by Rontani et al. (2019) on surface sediments shows that IPSO₂₅ may potentially be affected by autoxidative and bacterial degradation but oxidation products are found in only minor proportions. In general, further investigations into degradation processes affecting both HBIs and sterols within sediments would address an important knowledge gap regarding in-situ biochemical modifications of the biomarker signal. ¶ The δ¹³C values of IPSO₂₅ are between -10.3‰ and -14.7‰ which is the commonly observed range for IPSO₂₅ in surface sediments and sea ice derived organic matter (Massé et al., 2011, Belt et al., 2016), and contrasts the low δ¹³C values of [1]

Gelöscht: (Belt et al., 2015; Collins et al., 2013), we observe highest concentrations of the Z- and E-triene at the permanently ice-free northernmost stations in the eastern Drake Passage. This is also apparent for brassicasterol and dinosterol supporting an open marine (pelagic) source for... [2]

[1] nach unten verschoben: Elevated concentrations of both sterols in the Bransfield Strait could either point to an additional input of these lipids from melting sea ice (Belt et al., 2013) or a better adaptation of some of their source organisms to cooler and/or ice-

Gelöscht: dominated ocean conditions.

[2] nach unten verschoben: Production and accumulation of these lipids in (late) summer (i.e.

Gelöscht: Since brassicasterol and dinosterol are highly abundant in both seasonally ice-covered Bransfield Strait sediments as well as in permanently ice-free Drake Passage sediments, their use as an indicator of fully open-marine conditions is questionable.

Gelöscht: after the sea ice season) may be considered as well. This observation highlights the need for a better understanding of the source organisms and the mechanisms involved in the synthesis of these sterols.

1 Antarctic sediments (-38 ‰ to -41 ‰ after Massé et al., 2011) and support the sea ice origin of IPSO₂₅ in the study
2 area.

4 *Distribution of HBI trienes*

5 The HBI Z-triene was present in all 26 samples (0.33-26.86 µg g⁻¹ TOC) and the HBI E-triene was found in 24
6 samples (0.15-13.87 µg g⁻¹ TOC) (Table 1). Highest concentrations of both HBI trienes are found in the eastern

7 Drake Passage and along the continental slope, where IPSO₂₅ is absent, while their concentrations in the Bransfield
8 Strait are generally low (Fig. 3b and c) suggesting unfavorable environmental conditions for their producers (e.g.,

9 cooler SSTs, sea ice cover, grazing pressure) for their source diatoms. Contrary to the finding of elevated HBI Z-
10 triene concentrations in surface waters along an ice-edge (Smik et al., 2016a) and earlier suggestions that this

11 biomarker may be used as a proxy for MIZ conditions, (Belt et al., 2015; Collins et al., 2013; Schmidt et al., 2018),
12 we observe highest concentrations of the HBI Z- and E-triene at the permanently ice-free northernmost stations

13 PS97/083 and PS97/084 in the eastern Drake Passage. These core sites are located in close vicinity to the Polar
14 Front (Fig. 2) and we assume that the productivity of HBI triene source diatoms may benefit from mixing and

15 upwelling of warm and cold water masses in this area (Moore and Abbott, 2002). Sediments collected south of the
16 Polar Front and along the Hero Fracture Zone in the western Drake Passage (Fig. 2) contain moderate and very

17 low concentrations of HBI trienes, respectively. The Hero Fracture Zone is mainly barren of fine-grained
18 sediments and dominated by sands (Lamy, 2016), which may point to intensive winnowing by ocean currents

19 impacting the deposition and burial of organic matter. Moderate concentrations of HBI trienes at the continental
20 slope along the WAP (PS97/053, PS97/074, PS97/077) and in the Bransfield Strait likely refer to primary

21 production associated with the retreating sea ice margin during spring and summer. This indicates seasonally ice-
22 free waters in high production coastal areas influenced by upwelling (Gonçalves-Araujo et al., 2015) and feeding

23 of the local food web (Schmidt et al., 2018). The similarity in the distribution of the HBI Z- and the E-triene in
24 our surface sediments – the latter of which so far is not often considered for Southern Ocean paleoenvironmental

25 studies – supports the assumption of a common diatom source for these HBIs (Belt et al., 2000, 2017).

26 We consider that degradation of biomarker lipids may affect their distribution within surface sediments. While
27 laboratory studies on HBIs in solution point to a low reactivity of IPSO₂₅ towards auto- and photooxidative

28 degradation (Rontani et al., 2014, 2011), a more recent investigation into Antarctic surface sediments shows that
29 IPSO₂₅ may potentially be affected by partial autoxidative and bacterial degradation but oxidation products are

30 found in only minor proportions (Rontani et al., 2019a). Since HBI trienes exhibit a generally higher sensitivity to
31 degradation than the C₂₅ HBI diene (Rontani et al., 2014, 2019b) - and this is supported by a recent observation

1 of increasing IPSO₂₅/HBI triene ratios with increasing water depths in a polynya system off Eastern Antarctica
2 (Rontani et al., 2019b) – their lower concentrations in the Bransfield Strait have to be considered with care. Vice
3 versa, regarding maximum HBI triene concentrations and the absence of IPSO₂₅ in Drake Passage sediments, we
4 conclude that the absence of the latter in these samples can be linked to the lack of sea ice (and not to the
5 degradation of IPSO₂₅ as HBI trienes would have been removed first).

7 *Distribution of sterols*

8 Brassicasterol is present in all samples with concentrations ranging from 3.39 to 5017.44 µg g⁻¹ TOC, while
9 dinosterol was detected in 22 samples (0.0002-1983.75 µg g⁻¹ TOC). It is noticeable that the concentrations of
10 sterols exceed the concentrations of IPSO₂₅ and HBI trienes by more than two orders of magnitude. We observe
11 higher concentrations of brassicasterol and dinosterol in the eastern part of the Drake Passage supporting an open
12 marine source for these sterols. Surprisingly, elevated concentrations of brassicasterol are also found at stations
13 PS97/048-1 and 049-2 in the Hero Fracture Zone, which may argue against a winnowing signal leading to lower
14 accumulation of organic matter. We can only speculate if transport and deposition of reworked sediment
15 containing brassicasterol via iceberg rafting could explain these higher values. In contrast to the observation made
16 for HBI trienes, high sterol concentrations are found in the eastern and central Bransfield Strait (Fig. 3d and e).
17 Previously, elevated concentrations of steroidal components including brassicasterol and dinosterol in sediment
18 cores from the Bransfield Strait have been interpreted to reflect a high productivity and significant inputs from
19 diatoms and dinoflagellates (Brault and Simoneit, 1988). In a more recent overview, also Cárdenas et al. (2018)
20 report peak concentrations of pigments, sterols and total organic carbon in the Bransfield Strait, which they relate
21 to large seasonal phytoplankton blooms and higher accumulation rates. Dinosterol and, in particular, brassicasterol
22 are known to have different source organisms including diatoms, dinoflagellates, cryptophytes, prymnesiophycean
23 algae and cyanobacteria (Volkman, 1986) and we assume that this diversity accounts for the higher concentration
24 of these lipids in Bransfield Strait sediments, while concentrations of HBI trienes, mainly derived from diatoms,
25 are significantly lower. Regarding the potential input of brassicasterol from cryptophytes (Gladu et al., 1990; Goad
26 et al., 1983), changes in the dominance of this phytoplankton group over diatoms have been reported for our study
27 area and have been associated with a shallowing of the mixed layer and lower salinity due to intensified glacial
28 ice-melting along the WAP (Mendes et al., 2013).
29 Similar to the observations made for HBIs, selective degradation may also affect the concentration of phytosterols
30 within surface sediments. With respect to the preservation potential of terrigenous and marine derived sterols,
31 Rontani et al. (2012) note an only weak effect of biotic and abiotic degradation of brassicasterol in Arctic Ocean

Formatiert: Kopfzeile

1 shelf sediments – if this is also true for Southern Ocean shelf areas needs to be determined. In general, further
2 investigations into degradation processes affecting both HBIs and phytosterols within (the same) sediment samples
3 would address an important knowledge gap regarding in-situ biochemical modifications of the biomarker signal.

4.2 Comparison of satellite-derived modern sea ice conditions and biomarker data

4
5
6 The spring and winter sea ice concentrations are shown in Figure 4a and b. Winter sea ice is estimated to not
7 extend north of 61° S (Fig. 4b) and varies between 1 % and 50 % in the study area, while sea ice is reduced to less
8 than 20 % in spring (Fig. 4a, Table 2). Sea ice concentrations of up to 50 % are common in winter between the
9 South Shetland Islands and north of the Antarctic Sound where the influence of TWW is highest. Permanent sea
10 ice cover is uncommon in the Bransfield Strait and around the WAP and this area is mainly characterized by a
11 high sea ice seasonality, drift ice from the Weddell Sea (Collares et al., 2018) and a seasonally fluctuating sea ice
12 margin.

13 Comparisons of IPSO₂₅ and winter sea ice concentrations derived from satellite data reveal a positive correlation
14 ($r^2 = 0.53$). The strongest relationship is observed in the eastern Bransfield Strait where the influence of TWW is
15 high. Correlations with spring sea ice ($r^2 = 0.27$) and other seasons are weak. As photosynthesis is not possible
16 and a release of sea ice diatoms from melting sea ice is highly reduced during the Antarctic winter, the observation
17 of a stronger correlation between recent winter sea ice concentrations and IPSO₂₅ is unexpected. We hence suggest

18 that this offset may be related to the fact that the sediment samples integrate a longer time interval than is covered
19 by satellite observations. Radiocarbon dating of selected samples that contain calcareous material reveals an age
20 of 100 years BP in the vicinity of the South Shetland Islands (station PS97/059-2) and 142 years BP at the Antarctic
21 Sound (station PS1546-2, Table 3). A significantly older age was determined for a sample of *N. pachyderma* from
22 station PS97/044-1 (4830 years BP) which likely denotes the winnowing and/or very low sedimentation rates in
23 the Drake Passage. Bioturbation effects and uncertainties in reservoir ages potentially mask the ages of the near-

24 coastal samples. Nevertheless, since also other published ages of surface sediments within the Bransfield Strait
25 (Barbara et al., 2013; Barnard et al., 2014; Etourneau et al., 2013; Heroy et al., 2008) are in the range of 0-270
26 years, we consider that our surface samples likely reflect the paleoenvironmental conditions that prevailed during
27 the last two centuries (and not just the last 35 years covered by satellite observations). In the context of the rapid
28 warming during the last century (Vaughan et al., 2003) and the decrease of sea ice at the WAP (King, 2014; King
29 and Harangozo, 1998), we suggest that the biomarker data of the surface sediments relate to a spring sea ice cover,
30 which must have been enhanced compared to the recent (past 35 years) spring sea ice recorded via remote sensing.

31 Presumably, the average spring sea ice conditions over the past 200 years might have been similar to the modern

[3] verschoben (Einfügung)

[4] verschoben (Einfügung)

[5] verschoben (Einfügung)

[6] verschoben (Einfügung)

Formatiert: Kopfzeile

1 (past 35 years) winter conditions, which would explain the stronger correlation between IPSO₂₅ and winter sea ice
2 concentrations. The absence of IPSO₂₅ at stations PS97/052 and PS97/053, off the continental slope, is in conflict
3 with the satellite data depicting an average winter sea ice cover of 23 %. Earlier documentations that the IPSO₂₅
4 producing sea ice diatom *Berkeleya adeliensis* favors land-fast ice communities in East Antarctica and platelet ice
5 occurring mainly in near-coastal areas (Belt et al., 2016; Riaux-Gobin and Poulin, 2004) could explain this
6 mismatch between biomarker and satellite data, which further strengthens the hypothesis that the application of
7 IPSO₂₅ seems to be confined to continental shelf or near-coastal and meltwater affected environments (Belt, 2018;
8 Belt et al., 2016). Alternatively, strong ocean currents (i.e. the ACC) could have impacted the deposition of IPSO₂₅
9 in this region.

[7] verschoben (Einfügung)

10 Although the distribution pattern of HBI trienes reveals generally higher concentrations in ice-free environments,
11 we note only very weak negative correlations with satellite sea ice data ($r^2 < 0.1$). This may relate to the strong
12 spatial variability in HBI triene concentrations within the Drake Passage and the different time periods represented
13 by the satellite and sediment data. Similar to the HBI trienes, also the sterols do not show any significant
14 relationship to the satellite sea ice concentrations. High abundances of brassicasterol and dinosterol are observed
15 in both ice free as well as in seasonally ice-covered regions, which points to a broad environmental adaptation of
16 the source organisms. We hence consider that other environmental parameters than sea ice (e.g., nutrient
17 availability, water temperature and/or grazing pressure) exert a major control on the productivity of HBI triene
18 and sterol producers in the study area.

20 4.3 Comparison of biomarker distributions and diatom-based sea ice estimates

21 The diatoms preserved in sediments from the study area (Table 4) can be associated with open ocean and sea ice
22 conditions (Fig. 5a-d). North of the South Shetland Islands, the strong influence of the ACC is reflected in the high
23 abundance of open ocean diatom species such as *Fragilariopsis kerguelensis* and *Thalassiosira lentiginosa* (Esper
24 et al., 2010). The two diatom species *Fragilariopsis curta* and *Fragilariopsis cylindrus* – known to not produce
25 HBI_s (Belt et al., 2016; Sinninghe Damsté et al., 2004) - mark the vicinity to sea ice (Buffen et al., 2007; Pike et
26 al., 2008) and indicate fast and melting ice, a stable sea ice margin and stratification due to melting processes and
27 the occurrence of seasonal sea ice. These observations are in accordance with previous diatom studies revealing a
28 dominance of *Fragilariopsis kerguelensis* in the permanently open-ocean zone in the Drake Passage and an
29 assemblage shift to more cold water adapted and sea ice-associated species in the seasonal sea ice zone of the
30 Bransfield Strait (Cárdenas et al., 2018).

[8] verschoben (Einfügung)

[9] verschoben (Einfügung)

1 The high abundance of these sea ice diatoms in our samples is in good agreement with high and moderate IPSO₂₅
2 concentrations in the Bransfield Strait and around the South Shetland Islands, respectively. The only HBI source
3 diatom identified is the HBI Z-triene producing *Rhizosolenia hebetata* (Belt et al., 2017), which is present in four
4 samples in relatively small amounts which do not show a relation to the measured HBI Z-triene concentrations
5 (Table 1 and 4). The source diatom of IPSO₂₅ *Berkeleya adeliensis* was not observed (or preserved) in the samples,
6 and we suggest that additional, hitherto unknown, producers for IPSO₂₅ as well as for the HBI trienes may exist.
7 We applied the transfer function of Esper and Gersonde (2014a) with four analogs (4a, Table 4) to our samples
8 to estimate winter sea ice concentrations (WSI; Figure 5e). The diatom approach shows a clear trend of high winter
9 sea ice concentrations in the range of 78-91 % in the Bransfield Strait and low sea ice concentrations (between 6-
10 39 %) north of the continental slope. The fact that diatom data propose sea ice in the Drake Passage may result
11 from the high ages of surface sediments but also from drift, resuspension and sedimentation of diatom remains.
12 Because of the absence of IPSO₂₅ in the Drake Passage the correlation of its concentrations with WSI is only weak
13 ($r^2 = 0.29$).

15 4.4 Testing a semi-quantitative sea ice approach for the Southern Ocean: PIPSO₂₅

16 Following the PIP₂₅-approach applied in the Arctic Ocean (Müller et al., 2011; Belt and Müller, 2013; Xiao et al.,
17 2015), we used IPSO₂₅, HBI triene and sterol data to calculate the PIPSO₂₅ index. The main concept of combining
18 the sea ice proxy with an indicator of an ice-free ocean environment (i.e. a phytoplankton biomarker; Müller et al.,
19 2011), aims at a more detailed assessment of the sea ice conditions. By reducing the light penetration through the
20 ice, a thick and perennial sea ice cover limits the productivity of bottom sea ice algae (Hancke et al., 2018), which
21 results in the absence of both sea ice and pelagic phytoplankton biomarker lipids in the underlying sediments. Vice
22 versa, sediments from permanently ice-free ocean areas only lack the sea ice biomarker but contain variable
23 concentrations of phytoplankton biomarkers (Müller et al., 2011). The co-occurrence of both biomarkers in a
24 sediment sample suggests seasonal sea ice coverage promoting algal production indicative of sea ice as well as
25 open ocean environments (Müller et al., 2011). Consideration of a phytoplankton biomarker alongside the sea ice
26 proxy hence helps to avoid an underestimation of the past sea ice cover deduced from the absence of the sea ice
27 proxy, which, in fact, may also be due to a permanent sea ice cover (Belt, 2018, 2019; Belt and Müller, 2013).
28 Depending on the biomarker reflecting pelagic (open ocean) conditions, we here define P_ZIPSO₂₅ (using the HBI
29 Z-triene), P_EIPSO₂₅ (using the HBI E-triene), P_BIPSO₂₅ (using brassicasterol), and P_DIPSO₂₅ (using dinosterol).
30 The PIPSO₂₅ values are 0 in the Drake Passage and increase to intermediate values at the South Shetland Islands
31 and the continental slope and reach highest values in the Bransfield Strait (Fig. 6a-d). Minimum PIPSO₂₅ values

Formatiert: Kopfzeile

[10] verschoben (Einfügung)

[11] verschoben (Einfügung)

Gelöscht: ¶
A novel sea ice index

Formatiert: Englisch (Vereinigtes Königreich)

[12] verschoben (Einfügung)

Formatiert: Zeilenabstand: einfach

Gelöscht: (i.e. a phytoplankton biomarker, Müller et al., 2011), aims at a semi-quantitative assessment of the sea ice conditions.

[12] nach oben verschoben: Following the PIP₂₅-approach applied in the Arctic Ocean (Müller et al., 2011; Belt and Müller, 2013; Xiao et al., 2015), we used IPSO₂₅, HBI triene and sterol data to calculate the PIPSO₂₅ index.

Gelöscht: Depending on the biomarker reflecting pelagic (open ocean) conditions, we define P_ZIPSO₂₅ (using the Z-triene), P_EIPSO₂₅ (using the E-triene), P_BIPSO₂₅ (using brassicasterol), and P_DIPSO₂₅ (using dinosterol). Since the concentrations of IPSO₂₅ and both HBI trienes are in the same range, the application of the c-factor is not needed here. For the calculation of P_BIPSO₂₅ the c-factor is 0.0048, for P_DIPSO₂₅ it is 0.0137.¶

Gelöscht: 4a

1 are supposed to refer to a predominantly ice-free oceanic environment in the Drake Passage, while moderate
 2 PIPSO₂₅ values mark the transition towards a marginal sea ice coverage at the continental slope and around the
 3 South Shetland Islands. Elevated PIPSO₂₅ values in samples from the northeastern Bransfield Strait suggest an
 4 increased sea ice cover (probably sustained through the drift of sea ice originating in the Weddell Sea). This pattern
 5 reflects the oceanographic conditions of a permanently ice-free ocean north of the South Shetland Islands and a
 6 seasonal sea ice zone at the WAP influenced by the Weddell Sea as described by Cárdenas et al. (2018). Both HBI
 7 triene-based PIPSO₂₅ indices show constantly high values at the coast of the WAP of >0.7 (P_ZIPSO₂₅) and >0.8
 8 (P_EIPSO₂₅), respectively, and in the southern Bransfield Strait paralleling the southwest-northeast oriented
 9 Peninsula Front described by Sangrà et al. (2011). This front is reported to act as a barrier for phytoplankton
 10 communities (Gonçalves-Araujo et al., 2015) and is associated with the encounter between TWW carrying
 11 Weddell Sea sea ice through the Antarctic Sound and the TBW. The high PIPSO₂₅ values suggesting an extended
 12 sea ice cover west of the Peninsula Front (station PS97/054 and PS97/056) result from minimum concentrations
 13 of pelagic biomarkers and moderate concentrations of IPISO₂₅. PIPSO₂₅ values based on the HBI E-triene are about
 14 0.2 higher compared to P_ZIPSO₂₅, due to the generally lower concentrations of the HBI E-triene (Table 1).
 15 The sterol-based PIPSO₂₅ values display a generally similar pattern as P_ZIPSO₂₅ and P_EIPSO₂₅, respectively, and
 16 we note a high comparability between the P_EIPSO₂₅ and P_BIPSO₂₅ values (r² = 0.73). Some differences, however,
 17 are observed in the southwestern part of the Bransfield Strait (station PS97/056) where P_BIPSO₂₅ indicates a lower
 18 sea ice cover and in the central Bransfield Strait (stations PS97/068 and PS97/069) where P_BIPSO₂₅ and P_DIPSO₂₅
 19 point to only MIZ conditions. Regarding the modern sea ice conditions, the HBI triene-based PIPSO₂₅ indices
 20 hence seem to reflect the oceanographic conditions within the Bransfield Strait more satisfactorily. It has to be
 21 noted that the brassicasterol- or dinosterol-based PIPSO₂₅ index links environmental information derived from
 22 biomarker lipids belonging to different compound classes (i.e. HBIs and sterols), which have fundamentally
 23 different chemical properties. This requires special attention as, for example, selective degradation of one of the
 24 compounds may affect the sedimentary concentration of the respective lipids (Rontani et al., 2018). Previous
 25 studies linking HBI and sterol-based sea ice reconstructions with satellite-derived or, with respect to downcore
 26 paleo studies, paleoclimatic data, however, demonstrate that the climatic/environmental conditions controlling the
 27 production of HBIs and sterols seem to exceed the influence of a potential preferential degradation of these
 28 biomarkers within the sediments (e.g., Berben et al., 2014; Cabedo-Sanz et al., 2013; Müller et al., 2009, 2012;
 29 Müller and Stein, 2014; Stein et al., 2017; Xiao et al., 2015). A comparison of PIP₂₅ records determined using
 30 brassicasterol and the HBI Z-triene for three sediment cores from the Arctic realm covering the past up to 14.000
 31 years BP (Belt et al., 2015) reveals very similar trends for both versions of the PIP₂₅ index in each core, which

Formatiert: Kopfzeile

Gelöscht: slightly higher

Gelöscht: ↓

Gelöscht:

Formatiert: Zeilenabstand: einfach

Gelöscht: P_ZIPSO₂₅and

Gelöscht: reflect

Gelöscht: The

Gelöscht: -

Gelöscht:

Gelöscht: We note

Gelöscht: .

1 may point to, at least, a similar degree of degradation of HBI trienes and sterols through time. More such studies
 2 are needed to evaluate the preservation potential of HBIs and sterols in Southern Ocean sediments, especially for
 3 down core paleo studies.
 4 Since brassicasterol and dinosterol are highly abundant in both seasonally ice-covered Bransfield Strait sediments
 5 as well as in permanently ice-free Drake Passage sediments, their use as an indicator of fully open-marine
 6 conditions in the study area is questionable. Elevated concentrations of both sterols in the Bransfield Strait could
 7 either point to an additional input of these lipids from melting sea ice (Belt et al., 2013) or a better adaptation of
 8 some of their source organisms to cooler and/or ice-affected ocean environments. Production and accumulation of
 9 these lipids in (late) summer (i.e. after the sea ice season) has to be considered as well. This observation highlights
 10 the need for a better understanding of the source organisms and the mechanisms involved in the synthesis of these
 11 sterols. Similarly, more research is needed on the production of IPSO₂₅ in Southern Ocean sea ice environments.
 12 The source diatom *Berkeleya adeliensis* seems to be restricted to a very unique ice environment. Previous studies
 13 documenting the lack of IPSO₂₅ in distal though winter sea ice covered areas (e.g., Belt et al., 2016) emphasize
 14 this limitation and it has been suggested that IPSO₂₅ may be more indicative of the type of sea ice rather than sea
 15 ice extent (Belt, 2019), which needs to be considered when targeting at more quantitative sea ice reconstructions
 16 using this biomarker.
 17
 18 Comparison of PIPSO₂₅ with satellite, sea ice, data and diatom sea ice estimations.
 19 The contour lines in Figure 6a-d show the observed extent of 15 %, 30 %, 40 % and 50 % winter sea ice compared
 20 to the PIPSO₂₅ values. In the northeastern part of the study area, the HBI triene based PIPSO₂₅ indices align well
 21 with the contour lines of winter sea ice concentrations and depict the gradient from the marginally ice-covered
 22 southern Drake Passage towards the intensively ice-covered Weddell Sea. In the southwestern part of the
 23 Bransfield Strait, all PIPSO₂₅ indices suggest a higher sea ice cover than it is reflected in the satellite data. This
 24 may be explained by the transport (and melt) of drift ice through the TWW, joining the TBW at the southwestern
 25 Peninsula Front and/or a higher sea ice cover in this area prior to the remote sensing observational period (and
 26 prior to the recent WAP warming).
 27 Correlations of PIPSO₂₅ values with satellite-derived sea ice concentrations (for spring, summer, autumn and
 28 winter) contrast earlier observations made for the PIP₂₅ index in the Arctic Ocean, where the closest linear
 29 relationship is found mainly with the spring sea ice coverage (i.e. the blooming season of sea ice algae; Müller et
 30 al., 2011; Xiao et al., 2015). We observe a remarkably low correlation between PIPSO₂₅ values and spring sea ice
 31 concentrations of less than 20 % with a coefficient of determination $r^2 = 0.37$ for P₂IPSO₂₅, $r^2 = 0.50$ for P₁IPSO₂₅

Formatiert: Kopfzeile

Gelöscht: .

[1] verschoben (Einfügung)

[2] verschoben (Einfügung)

Formatiert: Zeilenabstand: einfach

Formatiert: Schriftart: Kursiv

Gelöscht: -derived modern

Formatiert: Schriftart: Kursiv

Gelöscht: conditions and biomarker

Formatiert: Schriftart: Kursiv

Formatiert: Schriftart: Kursiv

Formatiert: Schriftart: Kursiv

Formatiert: Standard, Block

[13] verschoben (Einfügung)

[3] nach oben verschoben: Winter sea ice is estimated to not extend north of 61° S (Fig.

Gelöscht: 4 f) and varies between 1 % and 50 % in the study area, while sea ice is reduced to less than 20 % in spring (Fig. 4e, Table 2). ¶

[4] nach oben verschoben: Sea ice concentrations of up to 50 % are common in winter between the South Shetland Islands and north of the Antarctic Sound where the influence of TWW is highest.

Gelöscht: Satellite-derived sea ice data were averaged over the time period from 1980 to 2015 for all four seasons (Table 2) and are considered to reflect the modern mean state of sea ice coverage around the WAP. The sea ice concentration is expressed to range from 0 to 100 % and, although the error can be up to 15 %, concentrations below 15 % still suggest the occurrence of sea ice. These low sea ice concentrations are usually neglected for the determination of the sea ice extent, which is defined as the ocean area with a sea ice cover of at least 15 %. The spring and winter sea ice concentrations are shown in Figure 4 e-f

Gelöscht: Permanent sea ice cover is uncommon in the Bransfield Strait and around the WAP and this area is mainly characterized by a high sea ice seasonality and drift ice from the Weddell Sea (Collares et al., 2018). Comparisons of individual biomarker concentrations with satellite sea ice data reveal a weak and positive correlation between IPSO₂₅ concentrations and winter sea ice concentrations ($r^2 = 0.5$), while no correlation is found between sea ice and pelagic biomarker concentrations ($r^2 < 0.1$ for all relations). ¶

Formatiert: Zeilenabstand: einfach

[14] verschoben (Einfügung)

(Fig. 7a), $r^2 = 0.31$ for $P_B\text{IPSO}_{25}$, and $r^2 = 0.34$ for $P_D\text{IPSO}_{25}$ (Fig. 7b). The highest correlation is observed between winter sea ice concentrations and $P_E\text{IPSO}_{25}$ ($r^2 = 0.72$), and $P_Z\text{IPSO}_{25}$ ($r^2 = 0.65$, Fig. 7c) with a weaker correlation for the sterol-based PIPSO_{25} values ($P_B\text{IPSO}_{25}$: $r^2 = 0.52$; $P_D\text{IPSO}_{25}$: $r^2 = 0.44$, Fig. 7d). As discussed above, we attribute this seemingly conflicting result of a better agreement between biomarker data and winter (instead of spring) sea ice conditions to the offset in the time intervals reflected in satellite and sediment data. For the application of the PIPSO_{25} approach, more aspects concerning the physical environmental conditions controlling the formation of platelet ice, which, at least at this state of research, is regarded as a main source of IPSO_{25} (Belt et al., 2016) need to be considered. The formation and accumulation of platelet ice in supercooled waters below landfast sea ice or underneath an ice-shelf (e.g., Gough et al., 2012; Hoppmann et al., 2015) seem to limit the spatial occurrence of IPSO_{25} and hence the applicability of PIPSO_{25} to coastal environments. However, transport of supercooled waters away from the coast may lead to platelet ice formation (and colonization of *Berkeleva adeliensis*) in more distal areas (Hoppmann et al., 2015) and also the drift of sea ice (including the underlying platelet ice) may impact the distribution of IPSO_{25} in Southern Ocean sediments and these processes require further investigations. Even though PIPSO_{25} values show a stronger relationship to satellite sea ice concentrations than IPSO_{25} concentrations more insight into the production and sedimentation of the involved biomarker lipids is needed to develop such a semi-quantitative approach.

With regard to the spatially and temporally variable sea ice extent, Esper and Gersonde (2014a) studied the response of diatom species to changes in environmental conditions and their response to the non-linear behavior of sea ice dynamics (Zwally et al., 2002). In contrast to ice free areas or areas of permanent sea ice cover, areas characterized by the transition from consolidated to unconsolidated sea ice show rapid changes in satellite derived sea ice concentrations (ranging from 90 % to 15 %) and exhibit a large variability in species composition. To reflect this curve in sea ice we hence chose a cubic polynomial regression (polynomial of third degree) to determine the relation between PIPSO_{25} values and satellite data depicting sea ice concentrations of more than 20 %. A slightly sigmoid-shaped regression line of winter sea ice concentrations and PIPSO_{25} values depicts the non-linearity of sea ice cover in different sea ice regimes.

A positive correlation is found between WSI concentrations derived from diatoms and the PIPSO_{25} indices based on HBI trienes ($P_Z\text{IPSO}_{25}$ with $r^2 = 0.76$; $P_E\text{IPSO}_{25}$ with $r^2 = 0.77$, Fig. 8a). The correlations of sterol-based PIPSO_{25} values with WSI are slightly lower but in the same range ($P_B\text{IPSO}_{25}$ with $r^2 = 0.74$; $P_D\text{IPSO}_{25}$ with $r^2 = 0.69$, Fig. 8b). A slightly weaker correlation is noted for diatom- and satellite-based winter sea ice concentrations ($r^2 = 0.63$; Fig. 8c). Overall, the diatom approach indicates higher sea ice concentrations than the satellite data with an offset of up to 65 %. This may be due to different sources of satellite reference data used for the transfer function or also

Formatiert: Kopfzeile

[15] verschoben (Einfügung)

Gelöscht: behaviour

[14] nach oben verschoben: We observe a remarkably low correlation between PIPSO_{25} values and spring sea ice concentrations of less than 20 % with a coefficient of determination $r^2 = 0.37$ for $P_Z\text{IPSO}_{25}$, $r^2 = 0.50$ for $P_E\text{IPSO}_{25}$ (Fig. 5).

Gelöscht: ¶

Gelöscht: 5a), $r^2 = 0.31$ for $P_B\text{IPSO}_{25}$, and $r^2 = 0.34$ for $P_D\text{IPSO}_{25}$ (Fig. 5b)

[15] nach oben verschoben:). The highest correlation is observed between winter sea ice concentrations and $P_E\text{IPSO}_{25}$ ($r^2 = 0.72$), and $P_Z\text{IPSO}_{25}$ ($r^2 = 0.65$, Fig. 5c).

Gelöscht: 5c). A weaker correlation is noted for the sterol-based PIPSO_{25} values ($P_B\text{IPSO}_{25}$: $r^2 = 0.52$; $P_D\text{IPSO}_{25}$: $r^2 = 0.44$, Fig. 5d). The

Gelöscht: reflects

Gelöscht: as mentioned above.

[13] nach oben verschoben: -d show the observed extent of 15 %, 30 %, 40 % and 50 % winter sea ice compared to the PIPSO_{25} values. In the northeastern part of the study area, the HBI triene based PIPSO_{25} indices align well with the contour lines of winter sea ice concentrations and depict the gradient from the marginally ice-covered southern Drake Passage towards the intensively ice-covered Weddell Sea. In the southwestern part of the Bransfield Strait, all PIPSO_{25} indices suggest a higher sea ice cover than it is reflected in the satellite data.

[5] nach oben verschoben: We hence suggest that this offset may be related to the fact that the sediment samples integrate a longer time interval than is covered by satellite observations. Radiocarbon dating of selected samples that contain calcareous material reveals an age of 100 years BP in the vicinity of the South Shetland Islands (station PS97/059-

Gelöscht: ¶

[6] nach oben verschoben: Nevertheless, since also other

[8] nach oben verschoben: North of the South Shetland

[9] nach oben verschoben: (Belt et al., 2016; Sinninghe

Gelöscht: The contour lines in Figure 4 a

[10] nach oben verschoben: The only HBI source diatom

[11] nach oben verschoben: We applied the transfer function

Gelöscht: This may be explained by the transport (and melt)

[7] nach oben verschoben: . Alternatively, strong ocean

Gelöscht: the ACC) could impact the deposition of IPSO_{25} (4)

Gelöscht: PIPSO_{25} sea ice estimates and winter sea ice ... [5]

Gelöscht: The two diatom species *Fragilariopsis curta* and [6]

Gelöscht: mark the vicinity to sea ice (Buffen et al., 2007; [7]

Gelöscht: rather small amounts and does not show a relation [8]

Gelöscht: compare the different estimates of sea ice cover [9]

Gelöscht: 6a

Gelöscht: 6b

Gelöscht: 6c

Formatiert: Kopfzeile

1 due to the fact that the sediment samples integrate a longer time period with a higher sea ice cover than the satellite
2 data (see discussion in section 4.2). Regarding future sea ice reconstructions based on IPSO₂₅ and other
3 biomarkers, we note that the simultaneous study of diatom assemblages provides valuable information on the sea
4 surface conditions and may help to avoid misleading interpretation of the biomarker data (Belt, 2019). Vice versa,
5 while diatom-based transfer functions mainly refer to winter sea ice concentrations, the IPSO₂₅ (and PIPSO₂₅)
6 signal holds critical information on coastal spring/summer sea ice conditions, which are often crucial for ice-shelf
7 (melting) processes. Pairing the micropaleontological and the biomarker approach hence provides for a more
8 comprehensive reconstruction of Southern Ocean sea ice conditions.

Gelöscht: 3).

Formatiert: Absatz-Standardschriftart, Schriftart: Fett, Schriftfarbe: Text 1

Formatiert: Kopfzeile

5 Conclusions

The distribution of the sea ice biomarker IPSO₂₅, related HBI trienes and **phytosterols** as well as diatoms in a suite of surface sediments from the southern Drake Passage and the WAP reflects recent sea **surface water characteristics** reasonably well. While highest HBI triene concentrations are observed in the permanently open ocean zone of the Drake Passage, they are significantly reduced in the seasonally ice-covered Bransfield Strait. This pattern is reversed for the sea ice proxy IPSO₂₅ and in accordance with previous surface sediment analyses revealing a preferential occurrence of this biomarker in near-coastal environments. The distribution of phytosterols points to a broader environmental significance of brassicasterol and dinosterol in terms of ocean temperature and sea ice tolerance, and/or nutrient availability. Following the PIP₂₅ approach established for Arctic Ocean sea ice reconstructions, the herein proposed sea ice index PIPSO₂₅ indicates seasonal sea ice cover along the coast of the WAP and in the Bransfield Strait, whereas mainly ice-free conditions prevail in the Drake Passage. In general, this pattern is consistent with satellite-derived sea ice data and diatom-based sea ice estimates and we note that the PIPSO₂₅ index seems a **potential** approach towards semi-quantitative sea ice reconstructions in the Southern Ocean. The recent rapid warming in the study area, however, affects the comparability of proxy and satellite data. The fact that the surface sediments integrate a significantly longer time interval than the remote sensing data thwarts attempts to calibrate PIPSO₂₅ values against observed sea ice concentrations. Additional data from other circum-Antarctic coastal (and distal) environments and investigations into potential calibration methods are needed to further develop this **approach**. Importantly, more information is needed on the mechanisms of IPSO₂₅ and HBI triene synthesis, transport and preservation within sediments. Despite a generally good agreement between PIPSO₂₅-, diatom- and satellite-based sea ice distributions, we note that the basically different sea ice patterns and sea ice varieties in the Southern Ocean and accordingly different mechanisms controlling the IPSO₂₅ signal need to be considered carefully, when adapting a (not yet fully validated) semi-quantitative approach initially developed for the Arctic Ocean.

Gelöscht: Application of PIPSO₂₅ as a semi-quantitative sea ice index

Precise and, in particular, quantitative reconstructions of past sea ice coverage are crucial for a robust assessment of feedback mechanisms in the ice-ocean-atmosphere system. While diatom transfer functions provide a valuable tool, additional information on sea ice conditions in coastal ice-shelf proximal areas, which are often affected by opal dissolution, are essential. The PIPSO₂₅ approach seems to be a promising step into this direction, though our data obtained for the WAP are not yet sufficient for a full calibration. PIPSO₂₅, diatom and satellite sea ice data, however, reveal positive correlations (Figs. 5 and 6) and depict similar gradients in sea ice cover. The observed offset between satellite data and biomarker- and diatom-based sea ice estimates likely relates to the fact that the instrumental records cover a significantly shorter or more recent time interval than the studied sediments. The recent rapid warming along the WAP (Vaughan et al., 2003) hence complicates attempts to calibrate these proxy data against observational data. Regarding the interpretation of PIPSO₂₅ in terms of sea ice coverage in the study area, lower PIPSO₂₅ values (<0.15 for P_ZIPSO₂₅; <0.31 for P_EIPSO₂₅; <0.22 for P_BIPSO₂₅ and P_DIPSO₂₅) roughly seem to reflect unconsolidated, drifting winter sea ice and a nearly ice-free spring season. Higher values (>0.71 for P_ZIPSO₂₅; >0.9 for P_EIPSO₂₅; >0.6 for P_BIPSO₂₅ and P_DIPSO₂₅) would refer to an extended winter sea ice cover (up to 91 % in some years) with ice floes remaining until summer.

Seitenumbruch

Gelöscht: Conclusion

Gelöscht: and

Gelöscht: sterols

Formatiert: Zeilenabstand: einfach

Gelöscht: ice conditions reasonably well. The

Gelöscht: promising

Gelöscht: index as a quantitative sea ice proxy.

Formatiert: Kopfzeile

1 **Data Availability**

2 All data can be found in this paper and will be available at the open access repository www.pangaea.de
3 (<https://doi.pangaea.de/10.1594/PANGAEA.897165>).

Gelöscht: .

Formatiert: Zeilenabstand: einfach

Formatiert: Schriftart: Nicht Kursiv

5 **Author contributions**

6 The study was conceived by MV and JM. Data collections and experimental investigations were done by MV
7 together with OE (diatoms), GM (radiocarbon dating), CH (satellite data), and ES (isotope data). MV wrote the
8 manuscript and did the visualizations. KF provided technical support. JM supervised the study. All authors
9 contributed to the interpretation and discussion of the results and the conclusion of this study.

Formatiert: Zeilenabstand: einfach

11 **Competing interests**

12 None of the authors has a conflict of interest.

14 **Acknowledgement**

15 We thank the captain, crew and chief scientist Frank Lamy of RV Polarstern cruise PS97, and the following
16 supporters: Mandy Kiel and Denise Diekstatt (technicians), Lester Lembke-Jene (biology, dating), Liz Bonk and
17 Hendrik Grotheer (from MICADAS), Max Mues (sample preparation), Nicoletta Ruggieri (lab support), Walter
18 Luttmmer (lab support). Simon Belt is acknowledged for providing the 7-HND internal standard for HBI
19 quantification. We also acknowledge the two anonymous reviewers and the editor for their constructive and
20 detailed comments. Financial support was provided through the Helmholtz Research grant VH-NG-1101.

Gelöscht: (technician)

Formatiert: Kopfzeile

References

Armand, L. K. and Zielinski, U.: Diatom Species of the genus *Rhizosolenia* from Southern Ocean sediments: distribution and taxonomic notes, *Diatom Res.*, 16(2), 259–294, doi:10.1080/0269249X.2001.9705520, 2001.

Formatiert: Zeilenabstand: einfach

Formatiert: Englisch (USA)

Armand, L. K., Crosta, X., Romero, O. and Pichon, J.-J.: The biogeography of major diatom taxa in Southern Ocean sediments: 1. Sea ice related species, *Palaeogeogr. Palaeoclimatol. Palaeoecol.*, 223(1–2), 93–126, doi:10.1016/J.PALAEO.2005.02.015, 2005.

Arrigo, K. R., Worthen, D. L., Lizotte, M. P., Dixon, P. and Dieckmann, G.: Primary Production in Antarctic Sea Ice, *Science*, 276, 394–397, doi:10.1126/science.276.5311.394, 1997.

Barbara, L., Crosta, X., Schmidt, S. and Massé, G.: Diatoms and biomarkers evidence for major changes in sea ice conditions prior the instrumental period in Antarctic Peninsula, *Quat. Sci. Rev.*, 79, 99–110, doi:10.1016/j.quascirev.2013.07.021, 2013.

Barbara, L., Crosta, X., Leventer, A., Schmidt, S., Etourneau, J., Domack, E. and Massé, G.: Environmental responses of the Northeast Antarctic Peninsula to the Holocene climate variability, *Paleoceanography*, 31(1), 131–147, doi:10.1002/2015PA002785, 2016.

Bárcena, M. A., Gersonde, R., Ledesma, S., Fabrés, J., Calafat, A. M., Canals, M., Sierro, F. J. and Flores, J. A.: Record of Holocene glacial oscillations in Bransfield Basin as revealed by siliceous microfossil assemblages, *Antarct. Sci.*, 10(03), 269–285, doi:10.1017/S0954102098000364, 1998.

Barnard, A., Wellner, J. S. and Anderson, J. B.: Late Holocene climate change recorded in proxy records from a Bransfield Basin sediment core, Antarctic Peninsula, *Polar Res.*, 33(1), doi:10.3402/polar.v33.17236, 2014.

Belt, S. T.: Source-specific biomarkers as proxies for Arctic and Antarctic sea ice, *Org. Geochem.*, 125, 277–298, doi:10.1016/j.orggeochem.2018.10.002, 2018.

[Belt, S. T.: What do IP25 and related biomarkers really reveal about sea ice change?, *Quat. Sci. Rev.*, 204, 216–219, doi:10.1016/j.quascirev.2018.11.025, 2019.](#)

Formatiert: Englisch (USA)

[Belt, S. T. and Müller, J.: The Arctic sea ice biomarker IP 25 : a review of current understanding , recommendations for future research and applications in palaeo sea ice reconstructions, *Quat. Sci. Rev.*, 79, 9–25, doi:10.1016/j.quascirev.2012.12.001, 2013.](#)

Formatiert: Englisch (USA)

Formatiert: Zeilenabstand: einfach

Belt, S. T., Allard, W. G., Massé, G., Robert, J. M. and Rowland, S. J.: Highly branched isoprenoids (HBIs): Identification of the most common and abundant sedimentary isomers, *Geochim. Cosmochim. Acta*, 64(22), 3839–3851, doi:10.1016/S0016-7037(00)00464-6, 2000.

Formatiert: Kopfzeile

1 Belt, S. T., Masse, G., Rowland, S. J., Poulin, M., Michel, C. and Leblanc, B.: A novel chemical fossil of palaeo sea
2 ice : *IP 25*, *Org. Geochem.*, 38, 16–27, doi:10.1016/j.orggeochem.2006.09.013, 2007.

3 Belt, S. T., Brown, T. A., Ringrose, A. E., Cabedo-Sanz, P., Mundy, C. J., Gosselin, M. and Poulin, M.: Quantitative
4 measurement of the sea ice diatom biomarker IP25 and sterols in Arctic sea ice and underlying sediments:
5 Further considerations for palaeo sea ice reconstruction, *Org. Geochem.*, 62, 33–45,
6 doi:10.1016/J.ORGGEOCHEM.2013.07.002, 2013.

7 Belt, S. T., Brown, T. A., Ampel, L., Cabedo-Sanz, P., Fahl, K., Kocis, J. J., Massé, G., Navarro-Rodríguez, A., Ruan,
8 J. and Xu, Y.: An inter-laboratory investigation of the Arctic sea ice biomarker proxy IP25 in marine sediments:
9 key outcomes and recommendations, *Clim. Past*, 10(1), 155–166, doi:10.5194/cp-10-155-2014, 2014.

10 Belt, S. T., Cabedo-Sanz, P., Smik, L., Navarro-Rodríguez, A., Berben, S. M. P., Knies, J. and Husum, K.:
11 Identification of paleo Arctic winter sea ice limits and the marginal ice zone: Optimised biomarker-based
12 reconstructions of late Quaternary Arctic sea ice, *Earth Planet. Sci. Lett.*, 431, 127–139,
13 doi:10.1016/j.epsl.2015.09.020, 2015.

14 Belt, S. T., Smik, L., Brown, T. A., Kim, J. H., Rowland, S. J., Allen, C. S., Gal, J. K., Shin, K. H., Lee, J. I. and Taylor,
15 K. W. R.: Source identification and distribution reveals the potential of the geochemical Antarctic sea ice proxy
16 IPSO25, *Nat. Commun.*, 7, 1–10, doi:10.1038/ncomms12655, 2016.

17 Belt, S. T., Brown, T. A., Smik, L., Tatarek, A., Wiktor, J., Stowasser, G., Assmy, P., Allen, C. S. and Husum, K.:
18 Identification of C25 highly branched isoprenoid (HBI) alkenes in diatoms of the genus *Rhizosolenia* in polar and
19 sub-polar marine phytoplankton, *Org. Geochem.*, 110, 65–72, doi:10.1016/j.orggeochem.2017.05.007, 2017.

20 Belt, S. T., Brown, T. A., Smik, L., Assmy, P. and Mundy, C. J.: Sterol identification in floating Arctic sea ice algal
21 aggregates and the Antarctic sea ice diatom *Berkeleya adeliensis*, *Org. Geochem.*, 118, 1–3,
22 doi:10.1016/j.orggeochem.2018.01.008, 2018.

23 Berben, S. M. P., Husum, K., Cabedo-Sanz, P. and Belt, S. T.: Holocene sub-centennial evolution of Atlantic
24 water inflow and sea ice distribution in the western Barents Sea, *Clim. Past*, 10(1), 181–198, doi:10.5194/cp-10-
25 181-2014, 2014.

26 [Brault, M. and Simoneit, B. R. T.: Steroid and triterpenoid distributions in bransfield strait sediments:
27 Hydrothermally-enhanced diagenetic transformations, *Org. Geochem.*, 13\(4–6\), 697–705, doi:10.1016/0146-
28 6380\(88\)90091-5, 1988.](#)

Formatiert: Englisch (USA)

29 [Buffen, A., Leventer, A., Rubin, A. and Hutchins, T.: Diatom assemblages in surface sediments of the](#)

Formatiert: Englisch (USA)

Formatiert: Zeilenabstand: einfach

- 1 northwestern Weddell Sea, Antarctic Peninsula, *Mar. Micropaleontol.*, 62(1), 7–30,
2 doi:10.1016/J.MARMICRO.2006.07.002, 2007.
- 3 Burckle, L. H. and Cooke, D. W.: Late Pleistocene *Eucampia antarctica* Abundance Stratigraphy in the Atlantic
4 Sector of the Southern Ocean, *Micropaleontology*, 29(1), 6, doi:10.2307/1485648, 1983.
- 5 Cabedo-Sanz, P., Belt, S. T., Knies, J. and Husum, K.: Identification of contrasting seasonal sea ice conditions
6 during the Younger Dryas, *Quat. Sci. Rev.*, 79, 74–86, doi:10.1016/j.quascirev.2012.10.028, 2013.
- 7 Cárdenas, P., Lange, C. B., Vernet, M., Esper, O., Srain, B., Vorrath, M.-E., Ehrhardt, S., Müller, J., Kuhn, G., Arz,
8 H. W., Lembke-Jene, L. and Lamy, F.: Biogeochemical proxies and diatoms in surface sediments across the
9 Drake Passage reflect oceanic domains and frontal systems in the region, *Prog. Oceanogr.*,
10 doi:10.1016/j.pocean.2018.10.004, 2018.
- 11 Cavaliere, D. J., Parkinson, C. L., Gloersen, P. and Zwally, H. J.: Sea Ice Concentrations from Nimbus-7 SMMR and
12 DMSP SSM/I-SSMIS Passive Microwave Data, Version 1, Boulder, Color. USA, doi:10.5067/8GQ8LZQVL0VL,
13 1996.
- 14 Collares, L. L., Mata, M. M., Kerr, R., Arigony-Neto, J. and Barbat, M. M.: Iceberg drift and ocean circulation in
15 the northwestern Weddell Sea, Antarctica, *Deep Sea Res. Part II Top. Stud. Oceanogr.*, 149(January 2019), 10–
16 24, doi:10.1016/j.dsr2.2018.02.014, 2018.
- 17 Collins, L. G., Allen, C. S., Pike, J., Hodgson, D. A., Weckström, K. and Massé, G.: Evaluating highly branched
18 isoprenoid (HBI) biomarkers as a novel Antarctic sea-ice proxy in deep ocean glacial age sediments, *Quat. Sci.*
19 *Rev.*, 79, 87–98, doi:10.1016/j.quascirev.2013.02.004, 2013.
- 20 Crosta, X., Pichon, J.-J. and Burckle, L. H.: Application of modern analog technique to marine Antarctic diatoms:
21 Reconstruction of maximum sea-ice extent at the Last Glacial Maximum, *Paleoceanography*, 13(3), 284–297,
22 doi:10.1029/98PA00339, 1998.
- 23 DeLaRocha, C. L. and Passow, U.: Factors influencing the sinking of POC and the efficiency of the biological
24 carbon pump, *Deep Sea Res. Part II Top. Stud. Oceanogr.*, 54(5–7), 639–658, doi:10.1016/j.dsr2.2007.01.004,
25 2007.
- 26 Denis, D., Crosta, X., Barbara, L., Massé, G., Renssen, H., Ther, O. and Giraudeau, J.: Sea ice and wind variability
27 during the Holocene in East Antarctica: insight on middle–high latitude coupling, *Quat. Sci. Rev.*, 29(27–28),
28 3709–3719, doi:10.1016/J.QUASCIREV.2010.08.007, 2010.
- 29 Esper, O. and Gersonde, R.: New tools for the reconstruction of Pleistocene Antarctic sea ice, *Palaeogeogr.*

1 Palaeoclimatol. Palaeoecol., 399, 260–283, doi:10.1016/J.PALAEO.2014.01.019, 2014a.
2 Esper, O. and Gersonde, R.: Quaternary surface water temperature estimations: New diatom transfer functions
3 for the Southern Ocean, Palaeogeogr. Palaeoclimatol. Palaeoecol., 414, 1–19,
4 doi:10.1016/J.PALAEO.2014.08.008, 2014b.
5 Esper, O., Gersonde, R. and Kadagies, N.: Diatom distribution in southeastern Pacific surface sediments and
6 their relationship to modern environmental variables, Palaeogeogr. Palaeoclimatol. Palaeoecol., 287(1–4), 1–
7 27, doi:10.1016/J.PALAEO.2009.12.006, 2010.
8 Etourneau, J., Collins, L. G., Willmott, V., Kim, J. H., Barbara, L., Leventer, A., Schouten, S., Sinninghe Damsté, J.
9 S., Bianchini, A., Klein, V., Crosta, X. and Massé, G.: Holocene climate variations in the western Antarctic
10 Peninsula: Evidence for sea ice extent predominantly controlled by changes in insolation and ENSO variability,
11 Clim. Past, 9(4), 1431–1446, doi:10.5194/cp-9-1431-2013, 2013.
12 [Fahl, K. and Stein, R.: Modern seasonal variability and deglacial/Holocene change of central Arctic Ocean sea-](#)
13 [ice cover: New insights from biomarker proxy records, Earth Planet. Sci. Lett., 351–352, 123–133,](#)
14 [doi:10.1016/j.epsl.2012.07.009, 2012.](#)
15 Fryxell, G. A. and Prasad, A. K. S. K.: *Eucampia antarctica* var. *recta* (Mangin) stat. nov. (Biddulphiaceae,
16 Bacillariophyceae): life stages at the Weddell Sea ice edge, Phycologia, 29(1), 27–38, doi:10.2216/i0031-8884-
17 29-1-27.1, 1990.
18 Fütterer, D. K.: Die Expedition ANTARKTIS-VI mit FS Polarstern 1987/1988 (The Expedition ANTARKTIS-VI of RV
19 Polarstern in 1987/88), Alfred-Wegener-Institut für Polar- und Meeresforschung, Bremerhaven, Germany.,
20 1988.
21 [Gersonde, R. and Zielinski, U.: The reconstruction of late Quaternary Antarctic sea-ice distribution — the use of](#)
22 [diatoms as a proxy for sea-ice, Palaeogeogr. Palaeoclimatol. Palaeoecol., 162, 263–286, doi:10.1016/S0031-](#)
23 [0182\(00\)00131-0, 2000.](#)
24 Gersonde, R., Crosta, X., Abelmann, A. and Armand, L.: Sea-surface temperature and sea ice distribution of the
25 Southern Ocean at the EPILOG Last Glacial Maximum—a circum-Antarctic view based on siliceous microfossil
26 records, Quat. Sci. Rev., 24(7–9), 869–896, doi:10.1016/J.QUASCIREV.2004.07.015, 2005.
27 [Gladu, P. K., Patterson, G. W., Wikfors, G. H., Chitwood, D. J. and Lusby, W. R.: The occurrence of brassicasterol](#)
28 [and epibrassicasterol in the chromophycota, Comp. Biochem. Physiol. Part B Comp. Biochem., 97\(3\), 491–494,](#)
29 [doi:10.1016/0305-0491\(90\)90149-N, 1990.](#)

Formatiert: Kopfzeile

Formatiert: Englisch (USA)

Formatiert: Zeilenabstand: einfach

Formatiert: Englisch (USA)

Formatiert: Englisch (USA)

1 [Gloersen, P., Campbell, W. J., Cavalieri, D. J., Comiso, J. C., Parkinson, C. L. and Zwally, H. J.: Arctic and antarctic](#)
2 [sea ice, 1978, *Ann. Glaciol.*, 17, 149–154, 1993.](#)

3 [Goad, L. J., Holz, G. G. and Beach, D. H.: Identification of \(24S\)-24-methylcholesta-5,22-dien-3 \$\beta\$ -ol as the major](#)
4 [sterol of a marine cryptophyte and a marine prymnesiophyte, *Phytochemistry*, 22\(2\), 475–476,](#)
5 [doi:10.1016/0031-9422\(83\)83028-3, 1983.](#)

6 [Gonçalves-Araujo, R., de Souza, M. S., Tavano, V. M. and Garcia, C. A. E.: Influence of oceanographic features](#)
7 [on spatial and interannual variability of phytoplankton in the Bransfield Strait, Antarctica, *J. Mar. Syst.*, 142, 1–](#)
8 [15, doi:10.1016/J.JMARSYS.2014.09.007, 2015.](#)

9 [Gough, A. J., Mahoney, A. R., Langhorne, P. J., Williams, M. J. M., Robinson, N. J. and Haskell, T. G.: Signatures](#)
10 [of supercooling: McMurdo Sound platelet ice, *J. Glaciol.*, 58\(207\), 38–50, doi:10.3189/2012jog10i218, 2012.](#)

11 [Hancke, K., Lund-Hansen, L. C., Lamare, M. L., Højlund Pedersen, S., King, M. D., Andersen, P. and Sorrell, B. K.:](#)
12 [Extreme Low Light Requirement for Algae Growth Underneath Sea Ice: A Case Study From Station Nord, NE](#)
13 [Greenland, *J. Geophys. Res. Ocean.*, 123\(2\), 985–1000, doi:10.1002/2017JC013263, 2018.](#)

14 [Hasle, G. R. and Syvertsen, E. E.: Marine diatoms, in *Identifying Marine Diatoms and Dinoflagellates*, edited by](#)
15 [C. R. Tomas, pp. 5–385, Academic Press Limited, London., 1996.](#)

16 [Heroy, D. C., Sjunneskog, C. and Anderson, J. B.: Holocene climate change in the Bransfield Basin, Antarctic](#)
17 [Peninsula: evidence from sediment and diatom analysis, *Antarct. Sci.*, 20\(01\), 69–87,](#)
18 [doi:10.1017/S0954102007000788, 2008.](#)

19 [Hobbs, W. R., Massom, R., Stammerjohn, S., Reid, P., Williams, G. and Meier, W.: A review of recent changes in](#)
20 [Southern Ocean sea ice , their drivers and forcings, *Glob. Planet. Change*, 143, 228–250,](#)
21 [doi:10.1016/j.gloplacha.2016.06.008, 2016.](#)

22 [Hofmann, E. E., Klinck, J. M., Lascara, C. M. and Smith, D. A.: Water mass distribution and circulation west of](#)
23 [the Antarctic Peninsula and including Bransfield Strait, in *Foundations for Ecological Research West of the*](#)
24 [Antarctic Peninsula, edited by R. . Ross, E. E. Hofmann, and L. B. Quetin, pp. 61–80, American Geophysical](#)
25 [Union \(AGU\), Washington, D. C., 1996.](#)

26 [Hoppmann, M., Nicolaus, M., Paul, S., Hunkeler, P. A., Heinemann, G., Willmes, S., Timmermann, R., Boebel, O.,](#)
27 [Schmidt, T., Kühnel, M., König-Langlo, G. and Gerdes, R.: Ice platelets below weddell sea landfast sea ice, *Ann.*](#)
28 [Glaciol., 56\(69\), 175–190, doi:10.3189/2015AoG69A678, 2015.](#)

29 [Kanazawa, A., Yoshioka, M. and Teshima, S.-I.: The occurrence of brassicasterol in the diatoms, *Cyclotella nana*](#)

Formatiert: Kopfzeile

Formatiert: Englisch (USA)

Formatiert: Zeilenabstand: einfach

Formatiert: Englisch (USA)

Formatiert: Englisch (USA)

Formatiert: Zeilenabstand: einfach

Formatiert: Englisch (USA)

Formatiert: Zeilenabstand: einfach

Formatiert: Englisch (USA)

Formatiert: Zeilenabstand: einfach

1 and Nitzschia closterium, Bull. Japanese Soc. Sci. Fish., 37, 889–903, 1971.

2 Kim, D., Kim, D. Y., Kim, Y. J., Kang, Y. C. and Shim, J.: Downward fluxes of biogenic material in Bransfield Strait,

3 Antarctica, Antarct. Sci., 16(3), 227–237, doi:10.1017/S0954102004002032, 2004.

4 [Kim, D., Kim, D. Y., Park, J. S. and Kim, Y. J.: Interannual variation of particle fluxes in the eastern Bransfield](#)

5 [Strait, Antarctica: A response to the sea ice distribution, Deep. Res. Part I Oceanogr. Res. Pap., 52\(11\), 2140–](#)

6 [2155, doi:10.1016/j.dsr.2005.06.008, 2005.](#)

7 [Kim, Y. S. and Orsi, A. H.: On the Variability of Antarctic Circumpolar Current Fronts Inferred from 1992–2011](#)

8 [Altimetry*, J. Phys. Oceanogr., 44\(12\), 3054–3071, doi:10.1175/jpo-d-13-0217.1, 2014.](#)

9 [King, J.: A resolution of the Antarctic paradox, Nature, 505\(7484\), 491–492, doi:10.1038/505491a, 2014.](#)

10 King, J. C. and Harangozo, S. A.: Climate change in the western Antarctic Peninsula since 1945: observations

11 and possible causes, Ann. Glaciol., 27, 571–575, doi:10.3189/1998AoG27-1-571-575, 1998.

12 Klunder, M. B., Laan, P., De Baar, H. J. W., Middag, R., Neven, I. and Van Ooijen, J.: Dissolved Fe across the

13 Weddell Sea and Drake Passage: impact of DFe on nutrient uptake, Biogeosciences, 11(3), 651–669,

14 doi:10.5194/bg-11-651-2014, 2014.

15 Lamy, F.: The expedition PS97 of the research vessel POLARSTERN to the Drake Passage in 2016, Reports Polar

16 Mar. Res., 7'01, 1–571, doi:10.2312/BzPM_0702_2016, 2016.

17 Leventer, A.: The fate of Antarctic “sea ice diatoms” and their use as paleoenvironmental indicators, in

18 Antarctic Research Series, edited by M. P. Lizotte and K. R. Arrigo, pp. 121–137, American Geophysical Union

19 (AGU), 1998.

20 Liu, J., Curry, J. A. and Martinson, D. G.: Interpretation of recent Antarctic sea ice variability, Geophys. Res.

21 Lett., 31(2), 2000–2003, doi:10.1029/2003GL018732, 2004.

22 Massé, G., Belt, S. T., Crosta, X., Schmidt, S., Snape, I., Thomas, D. N. and Rowland, S. J.: Highly branched

23 isoprenoids as proxies for variable sea ice conditions in the Southern Ocean, Antarct. Sci., 23(05), 487–498,

24 doi:10.1017/S0954102011000381, 2011.

25 [Mendes, C. R. B., Tavano, V. M., Leal, M. C., de Souza, M. S., Brotas, V. and Garcia, C. A. E.: Shifts in the](#)

26 [dominance between diatoms and cryptophytes during three late summers in the Bransfield Strait \(Antarctic](#)

27 [Peninsula\), Polar Biol., 36\(4\), 537–547, doi:10.1007/s00300-012-1282-4, 2013.](#)

28 Minzoni, R. T., Anderson, J. B., Fernandez, R. and Wellner, J. S.: Marine record of Holocene climate, ocean, and

29 cryosphere interactions: Herbert Sound, James Ross Island, Antarctica, Quat. Sci. Rev., 129, 239–259,

Formatiert: Kopfzeile

Formatiert: Englisch (USA)

Formatiert: Englisch (USA)

Formatiert: Englisch (USA)

Formatiert: Zeilenabstand: einfach

Formatiert: Englisch (USA)

Formatiert: Zeilenabstand: einfach

1 doi:10.1016/j.quascirev.2015.09.009, 2015.

2 [Moffat, C. and Meredith, M.: Shelf-ocean exchange and hydrography west of the Antarctic Peninsula: A review,](#)

3 [Philos. Trans. R. Soc. A Math. Phys. Eng. Sci., 376\(2122\), doi:10.1098/rsta.2017.0164, 2018.](#)

4 [Moore, J. K. and Abbott, M. R.: Surface chlorophyll concentrations in relation to the Antarctic Polar Front:](#)

5 [Seasonal and spatial patterns from satellite observations, J. Mar. Syst., 37\(1–3\), 69–86, doi:10.1016/S0924-](#)

6 [7963\(02\)00196-3, 2002.](#)

7 [Morrison, A. K., England, M. H. and Hogg, A. M.: Response of Southern Ocean Convection and Abyssal](#)

8 [Overturning to Surface Buoyancy Perturbations, J. Clim., 28\(10\), 4263–4278, doi:10.1175/JCLI-D-14-00110.1,](#)

9 [2015.](#)

10 [Müller, J. and Stein, R.: High-resolution record of late glacial and deglacial sea ice changes in Fram Strait](#)

11 [corroborates ice–ocean interactions during abrupt climate shifts, Earth Planet. Sci. Lett., 403, 446–455,](#)

12 [doi:10.1016/j.epsl.2014.07.016, 2014.](#)

13 [Müller, J., Massé, G., Stein, R. and Belt, S. T.: Variability of sea-ice conditions in the Fram Strait over the past](#)

14 [30,000 years, Nat. Geosci., 2\(11\), 772–776, doi:10.1038/ngeo665, 2009.](#)

15 [Müller, J., Wagner, A., Fahl, K., Stein, R., Prange, M. and Lohmann, G.: Towards quantitative sea ice](#)

16 [reconstructions in the northern North Atlantic: A combined biomarker and numerical modelling approach,](#)

17 [Earth Planet. Sci. Lett., 306\(3–4\), 137–148, doi:10.1016/J.EPSL.2011.04.011, 2011.](#)

18 [Müller, J., Werner, K., Stein, R., Fahl, K., Moros, M. and Jansen, E.: Holocene cooling culminates in sea ice](#)

19 [oscillations in Fram Strait, Quat. Sci. Rev., 47, 1–14, doi:10.1016/j.quascirev.2012.04.024, 2012.](#)

20 [Nichols, P. D., Volkman, J. K., Palmisano, A. C., Smith, G. A. and White, D. C.: Occurrence of an Isoprenoid C25](#)

21 [diunsaturated alkene and high neutral lipid content in Antarctic Sea-Ice Diatom communities, J. Phycol., 24, 90–](#)

22 [96, 1988.](#)

23 [Oksanen, J., Blanchet, F. G., Kindt, R., Legendre, P., Minchin, P. R., O’Hara, R. B., Simpson, G. L., Solymos, P.,](#)

24 [Stevens, M. H. H. and Wagner, H.: Vegan: Community Ecology Package \(R Package Version 2.0-3\), 2012.](#)

25 [Orsi, A. H., Whitworth, T. and Nowlin, W. D.: On the meridional extent and fronts of the Antarctic Circumpolar](#)

26 [Current, Deep. Res. Part I, 42\(5\), 641–673, doi:10.1016/0967-0637\(95\)00021-W, 1995.](#)

27 [Orsi, A. H., Smethie, W. M. and Bullister, J. L.: On the total input of Antarctic waters to the deep ocean: A](#)

28 [preliminary estimate from chlorofluorocarbon measurements, J. Geophys. Res., 107, 31-,](#)

29 [doi:10.1029/2001JC000976, 2002.](#)

Formatiert: Kopfzeile

Formatiert: Englisch (USA)

Formatiert: Englisch (USA)

Formatiert: Englisch (USA)

Formatiert: Zeilenabstand: einfach

Formatiert: Englisch (USA)

Formatiert: Zeilenabstand: einfach

Formatiert: Kopfzeile

1 [Pachauri, R. K., Mayer, L., Intergovernmental Panel on Climate Change, V. R., Broome, J., Cramer, W., Christ, R.,](#)
2 [Church, J. A., Clarke, L., Dahe, Q. D., Dasgupta, P., Dubash, N. K., Edenhofer, O., Elgizouli, I., Field, C. B., Forster,](#)
3 [P., Friedlingstein, P., Fuglestedt, J., Gomez-Echeverri, L., Hallegatte, S., Hegerl, G., Howden, M., Jiang, K.,](#)
4 [Cisneros, B. J., Kattsov, V., Lee, H., Mach, K. J., Marotzke, J., Mastrandrea, M. D., Meyer, L., Minx, J., Mulugetta,](#)
5 [Y., O'Brien, K., Oppenheimer, M., Pereira, J. J., Pichs-Madruga, R., Plattner, G.-K., Pörtner, H.-O., Power, S. B.,](#)
6 [Preston, B., Ravindranath, N. H., Reisinger, A., Riahi, K., Rusticucci, M., Scholes, R., Seyboth, K., Sokona, Y.,](#)
7 [Stavins, R., Stocker, T. F., Tschakert, P., Vuuren, D. van and Ypersele, J.-P. van: Climate change 2014 : synthesis](#)
8 [report, IPCC. \[online\] Available from: \[https://research-repository.uwa.edu.au/en/publications/climate-change-\]\(https://research-repository.uwa.edu.au/en/publications/climate-change-2014-synthesis-report-contribution-of-working-grou\)](#)
9 [2014-synthesis-report-contribution-of-working-grou \(Accessed 18 June 2019\), 2014.](#)

Formatiert: Englisch (USA)

10 Parkinson, C. L.: Trends in the length of the Southern Ocean sea-ice season, 1979-99, *Ann. Glaciol.*, 34(1), 435-
11 440, doi:10.3189/172756402781817482, 2002.

Formatiert: Zeilenabstand: einfach

12 Parkinson, C. L. and Cavalieri, D. J.: Antarctic sea ice variability and trends, 1979–2010, *Cryosph.*, 6, 871–880,
13 doi:10.5194/tc-6-871-2012, 2012.

14 Pike, J., Allen, C. S., Leventer, A., Stickley, C. E. and Pudsey, C. J.: Comparison of contemporary and fossil diatom
15 assemblages from the western Antarctic Peninsula shelf, *Mar. Micropaleontol.*, 67(3–4), 274–287,
16 doi:10.1016/J.MARMICRO.2008.02.001, 2008.

17 R Core Team: R: a Language and Environment for Statistical Computing, R Foundation for Statistical computing,
18 Vienna., 2012.

19 Ragueneau, O., Tréguer, P., Leynaert, A., Anderson, R. ., Brzezinski, M. ., DeMaster, D. ., Dugdale, R. ., Dymond,
20 J., Fischer, G., François, R., Heinze, C., Maier-Reimer, E., Martin-Jézéquel, V., Nelson, D. . and Quéguiner, B.: A
21 review of the Si cycle in the modern ocean: recent progress and missing gaps in the application of biogenic opal
22 as a paleoproductivity proxy, *Glob. Planet. Change*, 26(4), 317–365, doi:10.1016/S0921-8181(00)00052-7, 2000.

23 Reynolds, R. W., Rayner, N. A., Smith, T. M., Stokes, D. C., Wang, W., Reynolds, R. W., Rayner, N. A., Smith, T.
24 M., Stokes, D. C. and Wang, W.: An Improved In Situ and Satellite SST Analysis for Climate, *J. Clim.*, 15(13),
25 1609–1625, doi:10.1175/1520-0442(2002)015<1609:AIISAS>2.0.CO;2, 2002.

26 Reynolds, R. W., Smith, T. M., Liu, C., Chelton, D. B., Casey, K. S., Schlax, M. G., Reynolds, R. W., Smith, T. M.,
27 Liu, C., Chelton, D. B., Casey, K. S. and Schlax, M. G.: Daily High-Resolution-Blended Analyses for Sea Surface
28 Temperature, *J. Clim.*, 20(22), 5473–5496, doi:10.1175/2007JCLI1824.1, 2007.

29 Riaux-Gobin, C. and Poulin, M.: Possible symbiosis of *Berkeleya adeliensis* Medlin, *Synedropsis fragilis*

1 (Manguin) Hasle et al. and Nitzschia lecontei Van Heurck (bacillariophyta) associated with land-fast ice in
2 Adélie Land, Antarctica, Diatom Res., 19(2), 265–274, doi:10.1080/0269249X.2004.9705874, 2004.
3 Rintoul, S. R.: Rapid freshening of Antarctic Bottom Water formed in the Indian and Pacific oceans, Geophys.
4 Res. Lett., 34(6), L06606, doi:10.1029/2006GL028550, 2007.
5 Rontani, J.-F., Belt, S. T., Vaultier, F., Brown, T. A. and Massé, G.: Autoxidative and Photooxidative Reactivity of
6 Highly Branched Isoprenoid (HBI) Alkenes, Lipids, 49(5), 481–494, doi:10.1007/s11745-014-3891-x, 2014.
7 Rontani, J., Smik, L. and Belt, S. T.: Autoxidation of the sea ice biomarker proxy IPSO25 in the near-surface oxic
8 layers of Arctic and Antarctic sediments, Org. Geochem., 129, 63–76,
9 doi:10.1016/J.ORGEOCHEM.2019.02.002, [2019a](#).
10 [Rontani, J. F., Belt, S. T., Vaultier, F. and Brown, T. A.: Visible light induced photo-oxidation of highly branched](#)
11 [isoprenoid \(HBI\) alkenes: Significant dependence on the number and nature of double bonds, Org. Geochem.,](#)
12 [42\(7\), 812–822, doi:10.1016/j.orggeochem.2011.04.013, 2011.](#)
13 [Rontani, J. F., Charriere, B., Petit, M., Vaultier, F., Heipieper, H. J., Link, H., Chaillou, G. and Sempéré, R.:](#)
14 [Degradation state of organic matter in surface sediments from the Southern Beaufort Sea: A lipid approach,](#)
15 [Biogeosciences, 9\(9\), 3513–3530, doi:10.5194/bg-9-3513-2012, 2012.](#)
16 [Rontani, J. F., Belt, S. T. and Amiraux, R.: Biotic and abiotic degradation of the sea ice diatom biomarker IP25](#)
17 [and selected algal sterols in near-surface Arctic sediments, Org. Geochem., 118, 73–88,](#)
18 [doi:10.1016/j.orggeochem.2018.01.003, 2018.](#)
19 [Rontani, J. F., Smik, L., Belt, S. T., Vaultier, F., Armbrrecht, L., Leventer, A. and Armand, L. K.: Abiotic degradation](#)
20 [of highly branched isoprenoid alkenes and other lipids in the water column off East Antarctica, Mar. Chem.,](#)
21 [210, 34–47, doi:10.1016/j.marchem.2019.02.004, 2019b.](#)
22 [Sangrà, P., Gordo, C., Hernández-Arencibia, M., Marrero-Díaz, A., Rodríguez-Santana, A., Stegner, A., Martínez-](#)
23 [Marrero, A., Pelegrí, J. L. and Pichon, T.: The Bransfield current system, Deep Sea Res. Part I Oceanogr. Res.](#)
24 [Pap., 58\(4\), 390–402, doi:10.1016/J.DSR.2011.01.011, 2011.](#)
25 [Schmidt, K., Brown, T., Belt, S., Ireland, L., Taylor, K. W. R., Thorpe, S., Ward, P. and Atkinson, A.: Do pelagic](#)
26 [grazers benefit from sea ice? Insights from the Antarctic sea ice proxy IPSO25, Biogeosciences, 15\(7\), 1987–](#)
27 [2006, doi:10.5194/bg-15-1987-2018, 2018.](#)
28 Schrader, H. and Gersonde, R.: Diatoms and silicoflagellates, in Micropaleontological Methods and Techniques
29 An Exercise on an Eight Meter Section of the Lower Pliocene of Capo Rossello, Sicily, Utrecht

Formatiert: Kopfzeile

Gelöscht: 2019

Formatiert: Englisch (USA)

Formatiert: Englisch (USA)

Formatiert: Englisch (USA)

Formatiert: Englisch (USA)

Formatiert: Zeilenabstand: einfach

Formatiert: Englisch (USA)

Formatiert: Zeilenabstand: einfach

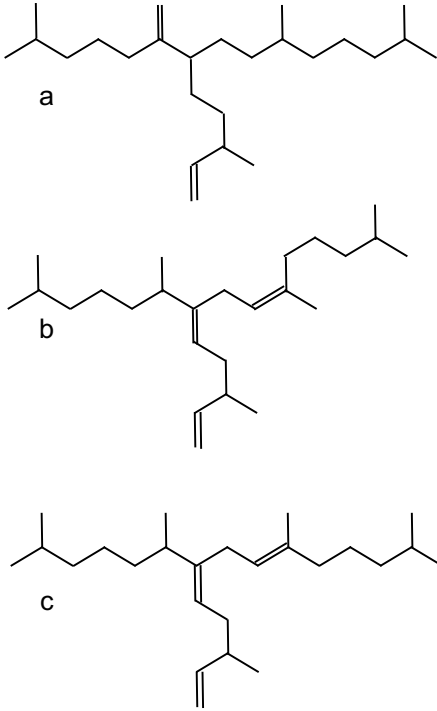
- 1 Micropaleontological Bulletins, vol. 17, edited by W. J. Zachariasse, W. R. Riedel, A. Sanfilippo, R. R. Schmidt, M.
2 J. Brolsma, H. J. Schrader, R. Gersonde, M. M. Drooger, and J. A. Broekman, pp. 129–176., 1978.
- 3 Simpson, G. L. and Oksanen, J.: Analogue: Analogue Matching and Modern Analogue Technique Transfer
4 Function Models. R Package Version 0.8-2, 2012.
- 5 Sinninghe Damsté, J. S., Muyzer, G., Abbas, B., Rampen, S. W., Massé, G., Allard, W. G., Belt, S. T., Robert, J. M.,
6 Rowland, S. J., Moldowan, J. M., Barbanti, S. M., Fago, F. J., Denisevich, P., Dahl, J., Trindade, L. A. F. and
7 Schouten, S.: The Rise of the Rhizosolenid Diatoms, *Science* (80-.), 304(5670), 584–587,
8 doi:10.1126/science.1096806, 2004.
- 9 Sinninghe Damsté, J. S., Rijpstra, W. I. C., Coolen, M. J. L., Schouten, S. and Volkman, J. K.: Rapid sulfuration of
10 highly branched isoprenoid (HBI) alkenes in sulfidic Holocene sediments from Ellis Fjord, Antarctica, *Org.*
11 *Geochem.*, 38(1), 128–139, doi:10.1016/j.orggeochem.2006.08.003, 2007.
- 12 Smik, L., Belt, S. T., Lieser, J. L., Armand, L. K. and Leventer, A.: Distributions of highly branched isoprenoid
13 alkenes and other algal lipids in surface waters from East Antarctica: Further insights for biomarker-based
14 paleo sea-ice reconstruction, *Org. Geochem.*, 95, 71–80, doi:10.1016/J.ORGGEOCHEM.2016.02.011, 2016a.
- 15 Smik, L., Cabedo-Sanz, P. and Belt, S. T.: Semi-quantitative estimates of paleo Arctic sea ice concentration
16 based on source-specific highly branched isoprenoid alkenes: A further development of the PIP 25 index, *Org.*
17 *Geochem.*, 92, 63–69, doi:10.1016/j.orggeochem.2015.12.007, 2016b.
- 18 Stein, R., Fahl, K. and Müller, J.: Proxy Reconstruction of Cenozoic Arctic Ocean Sea-Ice History: from IRD to
19 IP25, *Polarforschung*, 82(1), 37–71, 2012.
- 20 Stein, R., Fahl, K., Gierz, P., Niessen, F. and Lohmann, G.: Arctic Ocean sea ice cover during the penultimate
21 glacial and the last interglacial, *Nat. Commun.*, 8(1), 373, doi:10.1038/s41467-017-00552-1, 2017.
- 22 Stuiver, M., Reimer, P. J. and Reimer, R. W.: Calib 7.1, [online] Available from: <http://calib.org>, 2019.
- 23 Thompson, A. F., Heywood, K. J., Thorpe, S. E., Renner, A. H. H. and Trasiña, A.: Surface Circulation at the Tip
24 of the Antarctic Peninsula from Drifters, *J. Phys. Oceanogr.*, 39(1), 3–26, doi:10.1175/2008JPO3995.1, 2009.
- 25 Vaughan, D. G., Marshall, G. J., Connolley, W. M., Parkinson, C., Mulvaney, R., Hodgson, D. A., King, J. C.,
26 Pudsey, C. J. and Turner, J.: Recent Rapid Regional Climate Warming on the Antarctic Peninsula, *Clim. Change*,
27 60(3), 243–274, doi:10.1023/A:1026021217991, 2003.
- 28 Volkman, J. K.: A review of sterol markers for marine and terrigenous organic matter, *Org. Geochem.*, 9(2), 83–
29 99, doi:10.1016/0146-6380(86)90089-6, 1986.

- 1 Volkman, J. K.: Sterols in microorganisms, *Appl. Microbiol. Biotechnol.*, 60(5), 495–506, doi:10.1007/s00253-
2 002-1172-8, 2003.
- 3 Wacker, L., Bonani, G., Friedrich, M., Hajdas, I., Kromer, B., Němec, M., Ruff, M., Suter, M., Synal, H.-A. and
4 Vockenhuber, C.: MICADAS: Routine and High-Precision Radiocarbon Dating, *Radiocarbon*, 52(02), 252–262,
5 doi:10.1017/S0033822200045288, 2010.
- 6 Wefer, G., Fischer, G., Fütterer, D. and Gersonde, R.: Seasonal particle flux in the Bransfield Strait, Antarctica,
7 *Deep Sea Res. Part A. Oceanogr. Res. Pap.*, 35(6), 891–898, doi:10.1016/0198-0149(88)90066-0, 1988.
- 8 Wollenburg, J. E., Kettlein, C., Nehrke, G., Nöthig, E.-M., Matthiessen, J., Wolf- Gladrow, D. A., Nikolopoulos, A.,
9 Gázquez-Sánchez, F., Rossmann, L., Assmy, P., Babin, M., Bruyant, F., Beaulieu, M., Dybwad, C. and Peeken, I.:
10 Ballasting by cryogenic gypsum enhances carbon export in a *Phaeocystis* under-ice bloom, *Sci. Rep.*, 8(1), 7703,
11 doi:10.1038/s41598-018-26016-0, 2018.
- 12 Xiao, X., Fahl, K., Müller, J. and Stein, R.: Sea-ice distribution in the modern Arctic Ocean: Biomarker records
13 from trans-Arctic Ocean surface sediments, *Geochim. Cosmochim. Acta*, 155, 16–29,
14 doi:10.1016/J.GCA.2015.01.029, 2015.
- 15 Zielinski, U. and Gersonde, R.: Diatom distribution in Southern Ocean surface sediments (Atlantic sector):
16 Implications for paleoenvironmental reconstructions, *Palaeogeogr. Palaeoclimatol. Palaeoecol.*, 129(3–4), 213–
17 250, doi:10.1016/S0031-0182(96)00130-7, 1997.
- 18 Zielinski, U., Gersonde, R., Sieger, R. and Fütterer, D.: Quaternary surface water temperature estimations:
19 Calibration of a diatom transfer function for the Southern Ocean, *Paleoceanography*, 13(4), 365–383,
20 doi:10.1029/98PA01320, 1998.
- 21 Zwally, H. J., Comiso, J. C., Parkinson, C. L., Cavalieri, D. J. and Gloersen, P.: Variability of Antarctic sea ice 1979–
22 1998, *J. Geophys. Res.*, 107(C5), 3041, doi:10.1029/2000JC000733, 2002.
- 23

Formatiert: Kopfzeile

Formatiert: Zeilenabstand: einfach

1 Figures



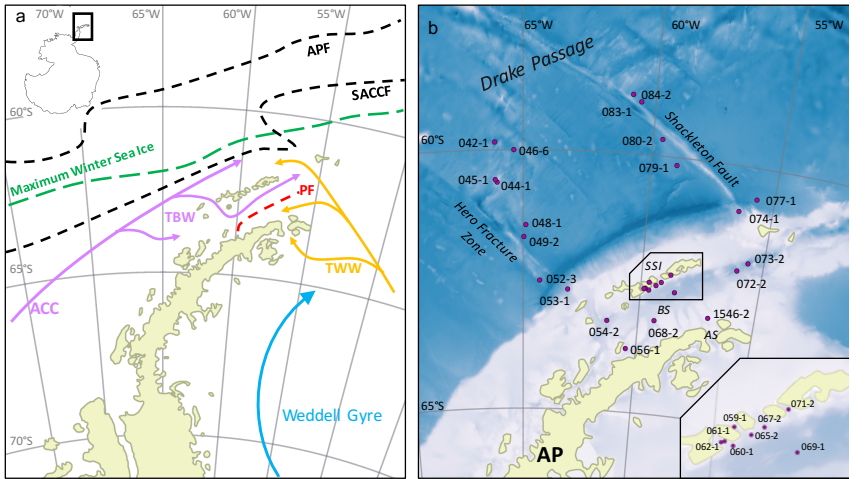
2

3 Figure 1: The molecular structures of a) IPSO₂₅, b) the HBI Z-triene, and c) the HBI E-triene.

4

Formatiert: Kopfzeile

1



2

Gelöscht:

Formatiert: Deutsch

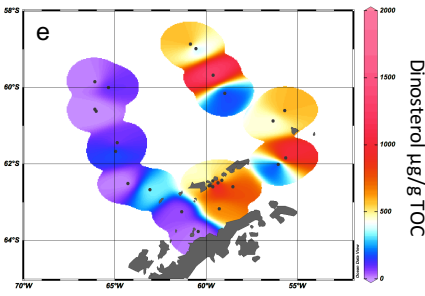
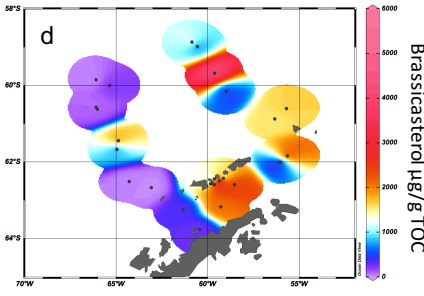
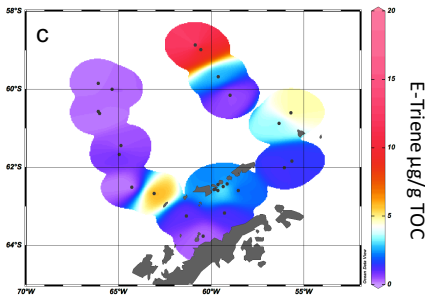
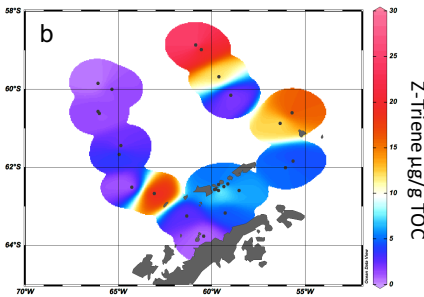
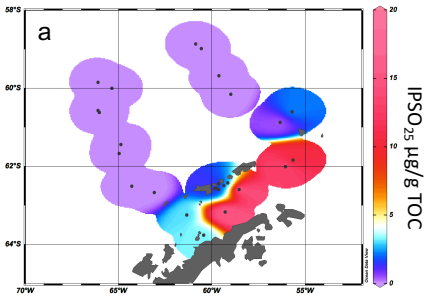
3 Figure 2: a) Oceanographic setting of the study area (modified after Hofmann et al., 1996; Sangrà et al., 2011) with
4 ACC = Antarctic Circumpolar Current, TBW = Transitional Bellingshausen Water, TWW = Transitional Weddell
5 Water, APF = Antarctic Polar Front, SACCF = Southern Antarctic Circumpolar Current Front, and PF = Peninsula
6 Front, and the maximum winter sea ice extent (after Cárdenas et al., 2018). b) The bathymetric map of the study area
7 with locations of all stations; AP = Antarctic Peninsula, AS = Antarctic Sound, BS = Bransfield Strait, and SSI = South
8 Shetland Islands. A detailed station map at the South Shetland Islands is integrated.

9 The overview maps were done with QGIS 3.0 from 2018 and the bathymetry was taken from GEBCO_14 from 2015.

10

Formatiert: Kopfzeile

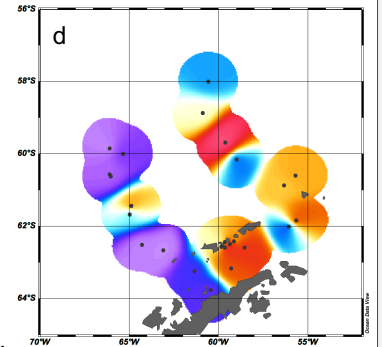
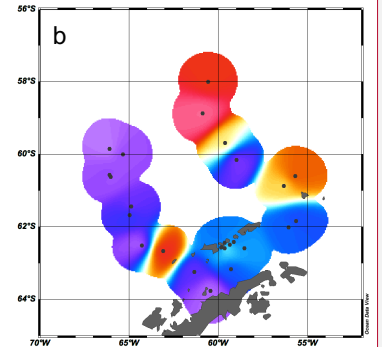
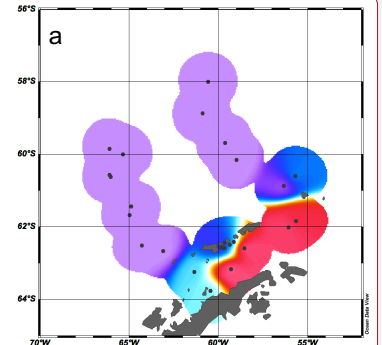
1



2

3 Figure 3: Distribution of a) IPSO₂₅, b) HBI Z-triene, c) HBI E-triene, d) brassicasterol, and e) dinosterol concentrations
4 normalized to TOC. All distribution plots were made with Ocean Data View 4.7.10 (2017).

5



Gelöscht:

Formatiert: Zeilenabstand: einfach

Formatiert: Kopfzeile

Formatiert: Zeilenabstand: einfach

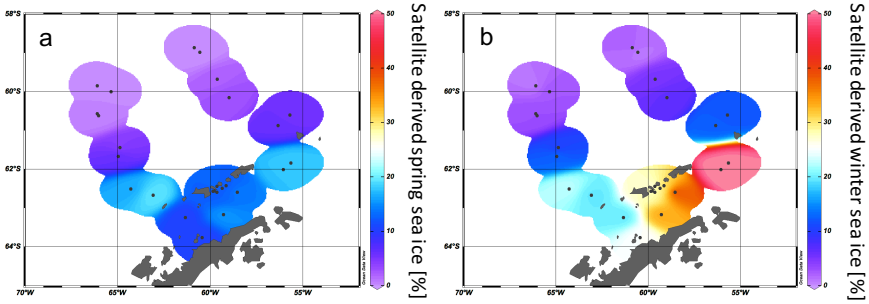
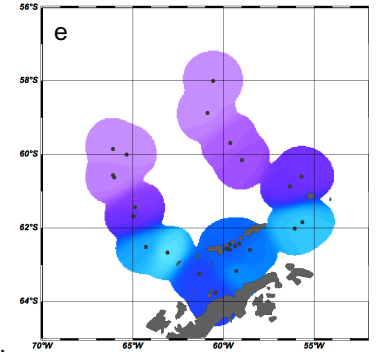
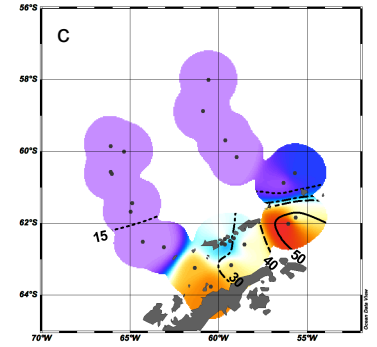
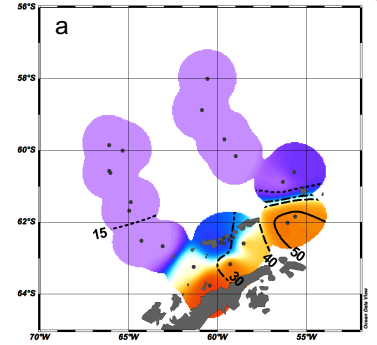
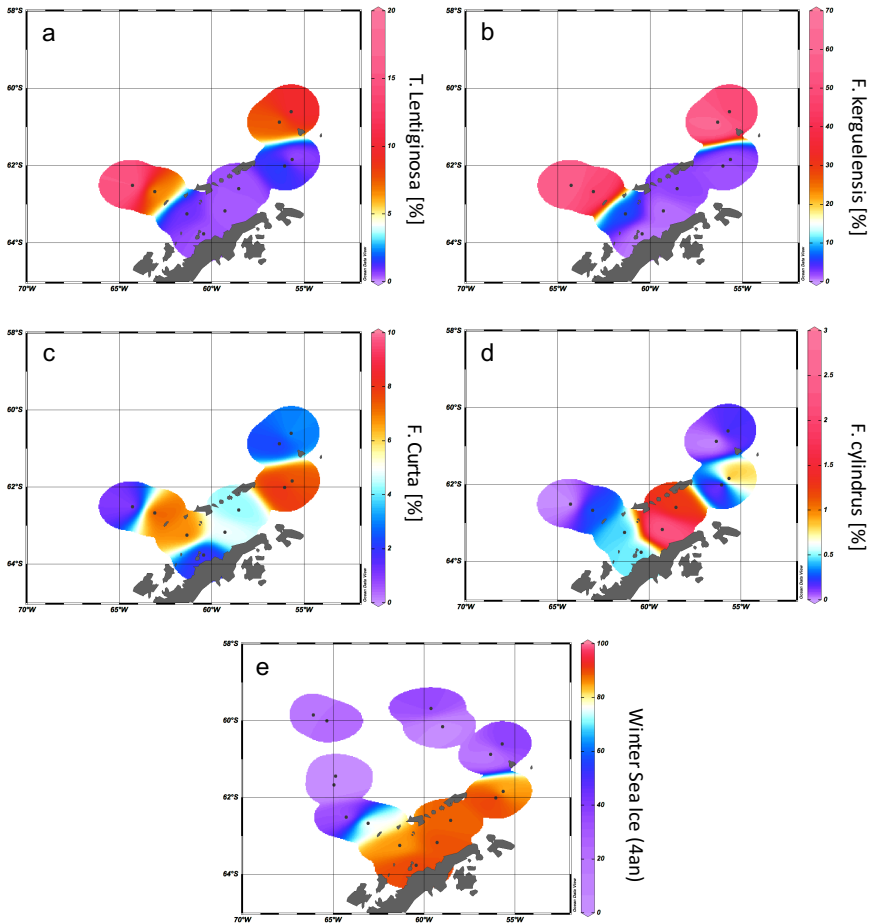


Figure 4: The satellite derived mean sea ice concentrations at each sampling station for a) spring and b) winter.

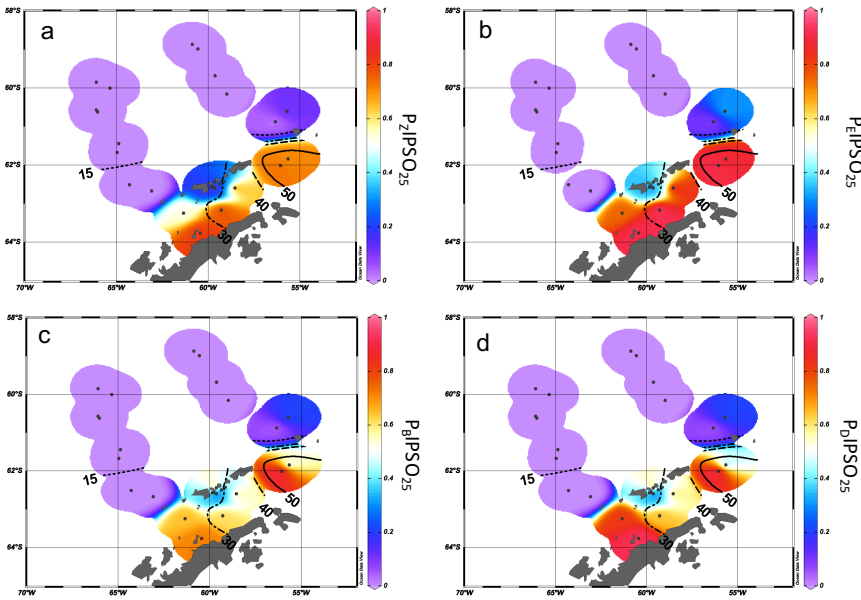


Gelöscht:

Formatiert: Deutsch



1
2 **Figure 5: Distribution of the diatoms a) *T. lentiginosa*, b) *F. kerguelensis*, c) *F. curta*, and d) *F. cylindrus* in the study**
3 **area (percentage per sample). The winter sea ice concentrations from the application of transfer function of Esper and**
4 **Gersonde (2014a) are shown in e).**
5



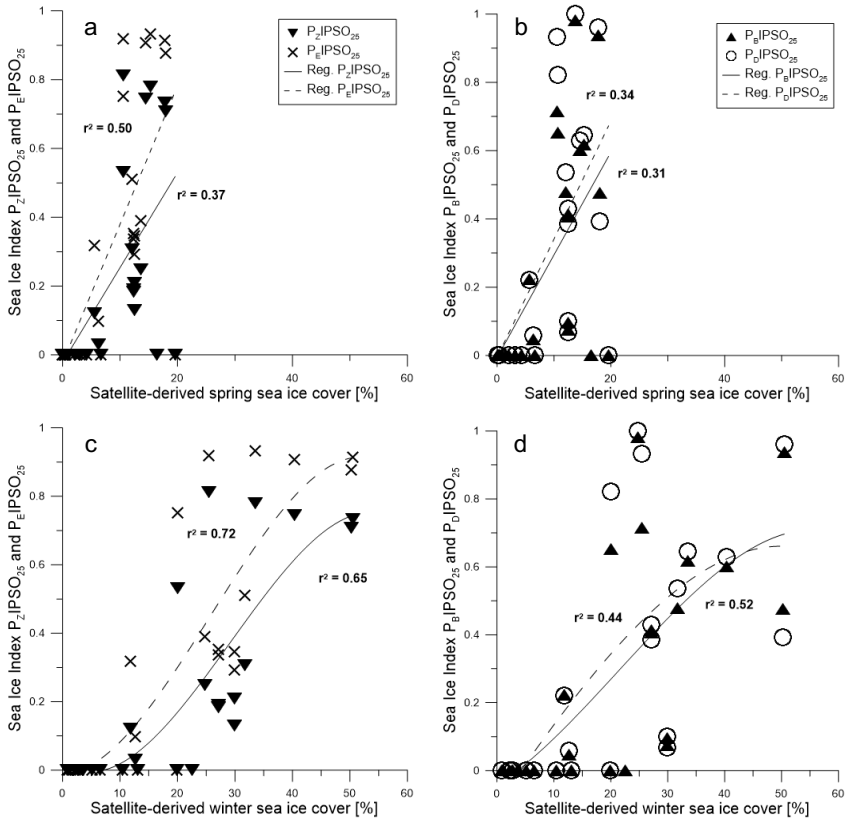
Formatiert: Kopfzeile

Formatiert: Zeilenabstand: einfach

Gelöscht: . Satellite derived mean sea ice concentrations at each sampling station are shown for e) spring and f) winter.

Gelöscht: ::::::::::::::::::::Seitenumbruch

1
2 **Figure 6:** Distribution of a) P_zIPSO_{25} , b) P_EIPSO_{25} , c) P_nIPSO_{25} , and d) P_DIPSO_{25} values in the study area. The extent
3 of 15 %, 30 %, 40 % and 50 % satellite sea ice concentrations during winter is added as contour lines (see also Figure
4 [4b](#)).



Formatiert: Kopfzeile

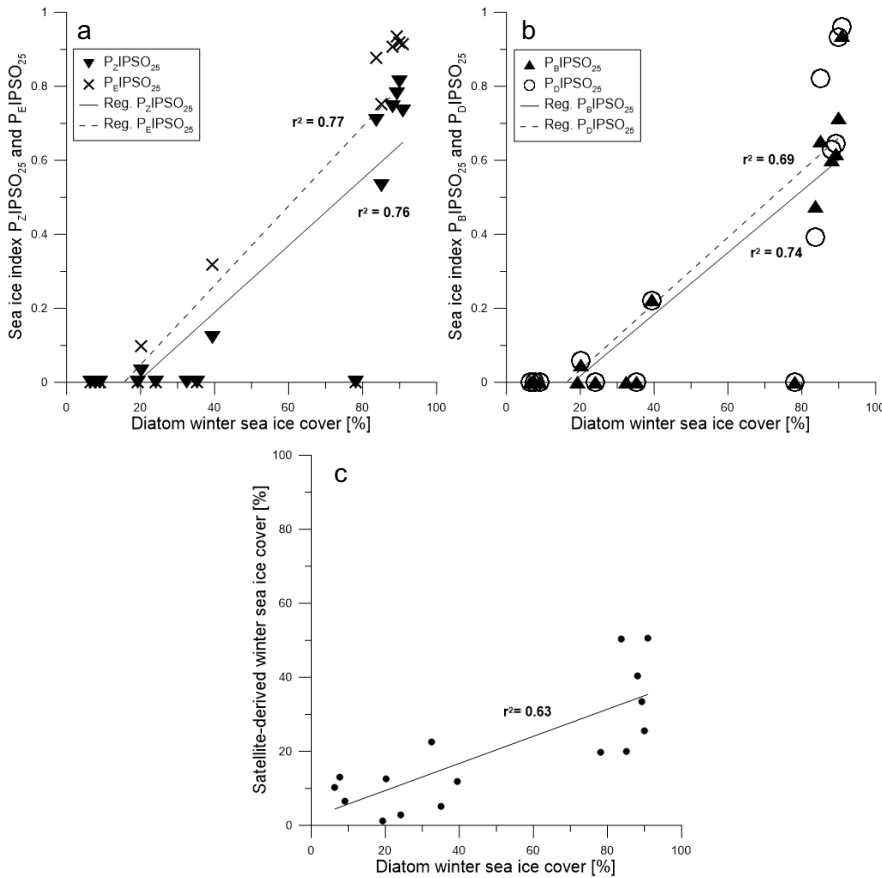
Formatiert: Zeilenabstand: einfach

Gelöscht: 5

Gelöscht: and

1
2
3
4
5
6
7

Figure 7: Scatter plots of satellite spring sea ice concentrations and a) P_ZIPSO₂₅ (triangles, solid regression line) and P_EIPSO₂₅ (crosses, dashed regression line) and b) P_BIPSO₂₅ (triangles, solid regression line) and P_DIPSO₂₅ (circles, dashed regression line). Scatter plots of satellite winter sea ice concentrations with c) P_ZIPSO₂₅ (triangles, solid regression line) and P_EIPSO₂₅ (crosses, dashed regression line) and d) P_BIPSO₂₅ (black triangles, solid regression line) and P_DIPSO₂₅ (circles, dashed regression line). All scatter plots were done with Grapher™ 13.



2

3 **Figure 8:** Scatter plots of a) P_zIPSO_{25} (triangles, solid regression line) and P_EIPSO_{25} (crosses, dashed regression line)
 4 and b) P_bIPSO_{25} (triangles, solid regression line) and P_DIPSO_{25} (circles, dashed regression line) against diatom derived
 5 winter sea ice concentrations. c) Scatter plot of diatom transfer function winter sea ice concentrations and satellite
 6 winter sea ice concentrations.

8 **Tables**

9 **Table 1: Coordinates of sample stations with water depth, concentrations of IPSO₂₅, HBI Z- and E-trienes, brassicasterol and dinosterol normalized to TOC, $\delta^{13}\text{C}$ values for IPSO₂₅, and**
10 **values of sea ice indices PIPSO₂₅ based on the HBI Z- and E-trienes, brassicasterol and dinosterol. Concentrations below the detection limit are expressed as 0. The PIPSO₂₅ could not be**
11 **calculated where IPSO₂₅ and the phytoplankton marker is absent (blank fields).**

Formati

Formati

Gelösch

Station	Lon [dE]	Lat [dN]	Water Depth [m]	HBI Z-Triene		HBI E-Triene		Brassicasterol	Dinosterol	δ ¹³ C of	IPSO ₂₅ [%]	P ₂ IPSO ₂₅	P ₁ IPSO ₂₅	P _B IPSO ₂₅	P _D IPSO ₂₅
				IPSO ₂₅ /TOC [μg/g TOC]											
PS97/042-1	-66.10	-59.85	4172	0	0.333	0.152	12.997	0	0.000	0.000	0.000	0.000	0.000	0.000	0.000
PS97/044-1	-66.03	-60.62	1203	0	1.080	0	143.688	0	0.000		0.000		0.000		0.000
PS97/045-1	-66.10	-60.57	2292	0	1.531	0.386	36.902	0	0.000	0.000	0.000	0.000	0.000	0.000	0.000
PS97/046-6	-65.36	-60.00	2803	0	1.359	0.291	214.634	101.809	0.000	0.000	0.000	0.000	0.000	0.000	0.000
PS97/048-1	-64.89	-61.44	3455	0	2.085	0.375	1859.609	73.532	0.000	0.000	0.000	0.000	0.000	0.000	0.000
PS97/049-2	-64.97	-61.67	3752	0	3.924	0.851	719.155	178.446	0.000	0.000	0.000	0.000	0.000	0.000	0.000
PS97/052-3	-64.30	-62.51	2890	0	0.679	0	26.554	0	0.000		0.000		0.000		0.000
PS97/053-1	-63.10	-62.67	2021	0	19.350	5.948	13.356	332.868	0.000	0.000	0.000	0.000	0.000	0.000	0.000
PS97/054-2	-61.35	-63.24	1283	3.033	2.675	1.000	337.686	48.579	-14.741	0.531	0.752	0.652	0.820	0.820	0.820
PS97/056-1	-60.45	-63.76	633	3.232	0.752	0.290	268.190	17.158	-10.3 ± 0.9	0.811	0.918	0.716	0.932	0.932	0.932
PS97/059-1	-59.66	-62.44	354	0.835	2.523	1.305	3.386	0.0002		0.249	0.390	0.981	0.999	0.999	0.999
PS97/060-1	-59.65	-62.59	462	1.934	12.937	4.693	5017.437	1983.750		0.130	0.292	0.074	0.066	0.066	0.066
PS97/061-1	-59.80	-62.56	467	1.018	4.341	1.870	302.356	119.512		0.190	0.352	0.413	0.383	0.383	0.383
PS97/062-1	-59.86	-62.57	477	0.907	4.044	1.787	276.372	88.272		0.183	0.337	0.407	0.428	0.428	0.428
PS97/065-2	-59.36	-62.49	480	2.416	9.184	4.549	4788.292	1587.309		0.208	0.347	0.095	0.100	0.100	0.100
PS97/067-2	-59.15	-62.42	793	1.785	4.038	1.710	406.567	113.728		0.307	0.511	0.478	0.533	0.533	0.533
PS97/068-2	-59.30	-63.17	794	16.206	4.558	1.152	2096.690	653.977	-14.1 ± 0.6	0.780	0.934	0.617	0.643	0.643	0.643

← **Formatiert: Kopfzeile**

Gelöscht: Brassi-casterol

Gelöscht: Dino-sterol

PS97/069-1	-58.55	-62.59	1642	17.814	6.115	1.824	2472.025	774.345	-12.6 ± 0.4	0.744	0.907	0.601	0.626
PS97/072-2	-56.07	-62.01	1992	13.689	4.997	1.277	192.625	40.686	-13.6 ± 0.3	0.733	0.915	0.937	0.961
PS97/073-2	-55.66	-61.84	2624	10.369	4.283	1.451	2388.458	1180.752		0.708	0.877	0.476	0.390
PS97/074-1	-56.35	-60.87	1831	0.371	12.075	3.409	1539.629	438.073		0.030	0.098	0.048	0.058
PS97/077-1	-55.71	-60.60	3587	2.267	16.356	4.874	1647.616	589.731		0.122	0.317	0.223	0.219
PS97/079-1	-59.00	-60.15	3539	0	1.893	0.510	479.917	154.400		0.000	0.000	0.000	0.000
PS97/080-2	-59.64	-59.68	3113	0	12.021	2.705	4019.003	1329.129		0.000	0.000	0.000	0.000
PS97/083-1	-60.57	-58.99	3756	0	18.256	8.280	686.502	308.610		0.000	0.000	0.000	0.000
PS97/084-2	-60.88	-58.87	3617	0	26.857	13.871	1245.652	648.474		0.000	0.000	0.000	0.000

Formatiert: Kopfzeile

Gelöscht: 00

Formatiert: Zeilenabstand: einfach

Formatiert: Kopfzeile

17 Table 2: Seasonal sea ice concentrations from satellite observations for spring, summer, autumn and winter with
18 standard deviations.

Station	Sea Ice	Sea Ice						
	Spring [%]	Spring StDev [%]	Summer [%]	Summer StDev [%]	Autumn [%]	Autumn StDev [%]	Winter [%]	Winter StDev [%]
PS97/042-1	0.04	0.19	0.00	0.00	0.01	0.05	1.14	5.00
PS97/044-1	0.92	3.25	0.02	0.23	0.00	0.00	3.67	9.38
PS97/045-1	0.52	2.08	0.01	0.08	0.00	0.04	2.65	7.81
PS97/046-6	0.29	1.35	0.00	0.00	0.00	0.00	2.84	8.55
PS97/048-1	4.22	8.52	0.00	0.00	0.00	0.00	10.36	18.17
PS97/049-2	6.65	11.85	0.00	0.00	0.00	0.04	13.02	19.91
PS97/052-3	16.48	21.62	0.40	2.95	0.04	0.31	22.59	24.94
PS97/053-1	19.59	23.59	0.29	2.45	0.04	0.35	19.86	24.13
PS97/054-2	10.62	15.18	0.44	0.79	0.76	2.62	20.06	20.72
PS97/056-1	10.55	16.21	4.73	3.25	2.77	4.44	25.47	23.02
PS97/059-1	13.67	16.13	4.23	2.25	5.03	5.48	24.77	20.33
PS97/060-1	12.53	16.84	1.87	2.15	5.43	9.24	29.93	22.05
PS97/061-1	12.43	16.18	1.86	2.07	4.15	7.30	27.14	21.31
PS97/062-1	12.43	16.18	1.86	2.07	4.15	7.30	27.14	21.31
PS97/065-2	12.53	16.84	1.87	2.15	5.43	9.24	29.93	22.05
PS97/067-2	12.08	17.22	0.82	1.88	5.60	10.10	31.74	22.69
PS97/068-2	15.30	19.35	4.89	3.40	6.44	10.45	33.49	23.13
PS97/069-1	14.51	19.85	0.40	2.34	7.83	13.78	40.41	24.27
PS97/072-2	17.74	22.74	1.46	5.38	16.69	20.35	50.49	25.09
PS97/073-2	17.99	23.28	1.81	6.14	16.43	19.85	50.29	26.01
PS97/074-1	6.30	13.65	0.02	0.12	0.55	2.29	12.65	19.30
PS97/077-1	5.60	12.20	0.04	0.13	0.77	2.99	11.83	17.81
PS97/079-1	3.10	8.91	0.03	0.27	0.01	0.12	6.50	15.49
PS97/080-2	2.08	7.52	0.01	0.08	0.00	0.04	5.14	14.17
PS97/083-1	0.03	0.23	0.00	0.00	0.00	0.04	0.87	4.27
PS97/084-2	0.40	2.21	0.00	0.00	0.00	0.04	2.23	9.59

Formatiert: Zeilenabstand: einfach

19

20 **Table 3: Details of the radiocarbon dates and calibrated ages.**

Sample Name	AWI-No.	Material	F ¹⁴ C ± error	Conventional ¹⁴ C age [a]	Calibrated age (cal BP) [a]
PS97/044-1	1657.1.1	N. pachyderma	0.5076	5447 ± 111	4830
PS97/059-2	1434.1.1	calcareous	0.8507	1299 ± 49	100
PS1546-2	1602.1.1	Moll.-Echinod	0.8456	1347 ± 64	142

← Formatiert: Kopfzeile

21

22

← Formatiert: Zeilenabstand: einfach

Table 4: Estimations of winter sea ice (WSI) derived from diatom species and the distribution of main diatom species in each sample.

Station	Diatoms WSI (4an) [%]	A. tabularis [%]	E. antarctica [%]	F. vanheurckii [%]	F. kerguelensis [%]	F. obliquecostata [%]	F. sublinearis [%]	F. curta [%]	F. cylindrus [%]	N. directa [%]	O. weissflogii [%]	P. lineola-turgid.-gr. [%]	R. alata [%]	R. hebetata fo. semispina [%]	S. microtrias [%]	T. lentiginosa [%]	T. oliverana [%]	Thalassiosira MT 3 [%]	P. pseudodenticulata [%]	Stephanopyxis sp. [%]
PS97/042-1	19.2	0	0	0	0.8	0	0	0	0	0	0	0	0	0	0	0	0	0	0	0
PS97/046-6	24.2	0	0	0	0.8	0	0	0	0	0	0	0	0	0	0	0	0	0	0	0
PS97/048-1	6.4	0	0	0	0.8	0	0	0	0	0	0	0	0	0	0	0	0	0	0	0
PS97/049-2	7.7	0	0	0	0.7	0	0	0	0	0	0	0	0	0	0	0	0	0	0	0
PS97/052-3	32.4	1.4	4.3	0	60.3	0.2	0	0.9	0	0	0.5	0	0	0	0	16.2	0.5	0	0	0
PS97/053-1	78.1	0.4	1.2	0	48.5	0.1	0.1	7.4	0.3	0	0.4	0	0.3	0	0.1	6.5	0	0	0	0
PS97/054-2	85.2	0	0.4	0	6.2	0	0	6.9	0.4	0.2	2.7	0.2	0.2	0.2	0.4	0.9	0	0.2	0	0.4
PS97/056-1	89.9	0	0	0	0.5	0.3	0	1.9	0.5	0.3	0.5	0	0	0	0.5	0.5	0	0.0	0.5	0.3
PS97/068-2	89.2	0	0	0	0.7	0.3	0.6	4.9	2.4	0.1	0.5	0.1	0	0	0.4	0.4	0	0.4	0.2	0
PS97/069-1	88.2	0	0.2	0.4	2.1	0.2	0.4	4.3	1.3	0	0.6	0.2	0	0	0.2	0.4	0	0.2	0	0
PS97/072-2	90.9	0	0.2	1.1	1.7	0.6	0.9	8.1	0	0	5.7	0.2	0.2	0	0	1.7	0	0.9	0.9	0
PS97/073-2	83.7	0	0.2	0.2	1.8	0	0.4	7.4	1.0	0	1.0	0	1.6	0.8	0	0.4	0	2.1	0.6	0
PS97/074-1	20.1	0.4	0.6	0	63.1	0	0	2.3	0	0	0.2	0	0.0	0.2	0	7.4	0.4	0	0.2	0
PS97/077-1	39.4	0.6	3.3	0	49.1	0.8	0	3.1	0.2	0	0.2	0	0.0	1.3	0	10.0	0.2	0	0	0

Formatiert: Kopfzeile

|

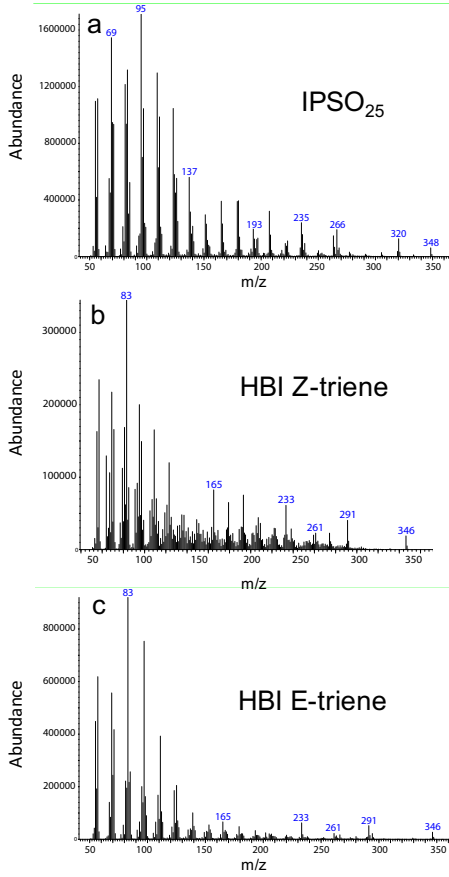
PS97/079-1	9.1	0	0	0	0.7	0	0	0	0	0	0	0	0	0	0	0	0	0	0	0	0
PS97/080-2	35.1	0	0	0	0.7	0	0	0	0	0	0	0	0	0	0	0	0	0	0	0	0

Formatiert: Kopfzeile

| 24

25

Supplementary Material



26

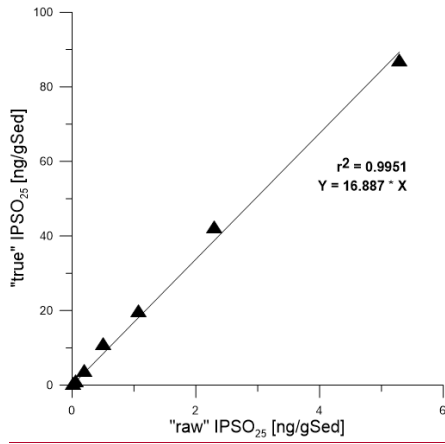
27 Supplement S1: Examples of mass spectra of IPSO₂₅ (m/z 348), HBI Z-triene and E-triene (both m/z 346)

28 obtained from surface sediments in the study area.

29

Formatiert: Kopfzeile

Formatiert: Links: 2.5 cm, Rechts: 2.5 cm, Oben: 2 cm,
Unten: 2.4 cm, Breite: 20.99 cm, Höhe: 29.7 cm



Formatiert: Kopfzeile

30

31 **Supplement S2: Example calibration curve for the quantification of IPSO₂₅. Different (true) IPSO₂₅**
 32 **concentrations determined via gas chromatography-flame ionization are plotted against (raw) IPSO₂₅**
 33 **concentrations determined via gas chromatography-mass spectrometry using selected ion monitoring (m/z**
 34 **348). The instrumental response factor is obtained from the regression line.**

Formatiert: Zeilenabstand: einfach

Formatiert: Schriftart: 10 Pt., Fett